

**IMPLEMENTATION OF A  
TWO PSEUDO-COMPONENT APPROACH  
FOR VARIABLE BUBBLE POINT PROBLEMS  
IN GPRS**

**A REPORT  
SUBMITTED TO THE DEPARTMENT OF ENERGY RESOURCES  
ENGINEERING  
OF STANFORD UNIVERSITY  
IN PARTIAL FULFILLMENT OF THE REQUIREMENTS  
FOR THE DEGREE OF  
MASTER OF SCIENCE**

**By  
Yi Wang  
June 2007**

I certify that I have read this report and that in my opinion it is fully adequate, in scope and in quality, as partial fulfillment of the degree of Master of Science in Petroleum Engineering.

---

Prof. Hamdi Tchelepi  
(Principal advisor)

# Abstract

The black-oil model is widely used in reservoir simulation. In this model, two pseudo components are used to represent the hydrocarbon system; a third component is used to represent water. In the standard black-oil model, the gas component is allowed to dissolve in the liquid oil phase. The point at which the mixture goes from single-phase liquid to two phases (i.e., liquid and gas) is called the bubble-point. There are many reservoir displacement processes where the bubble-point pressure is not necessarily constant. For example, in water-flooding operations of a depleted oil reservoir, it may be possible for all the free gas to dissolve as the pressure increases close to the injection site. In order to model variable bubble point problems in a black-oil formulation, special treatment is necessary. The black-oil model in the General Purpose Research Simulator (GPRS) was based on the assumption of constant bubble-point pressure throughout the simulation. In this report, we describe the extension for proper treatment of variable bubble-point problems. A Two Pseudo-Component Approach (TPCA) is used, in which the black-oil model is treated as a special compositional model with two hydrocarbon components, namely, oil and gas. The TPCA module, which is expected to replace the black-oil branch in GPRS completely, takes standard black-oil input data and translates them into compositional fluid properties. Then the black-oil simulation is actually carried out using the compositional code branch in GPRS, except that the equation-of-state computations are replaced by explicit expressions of the phase compositions. With the TPCA module and the reliable compositional treatment in GPRS, variable bubble point problems are handled correctly and efficiently.

# Acknowledgements

This project would not have been possible without the support of many people. First of all, many thanks to my advisor, Prof. Hamdi Tchelepi, who provided direction during my two-year Master program. Also thanks to Dr. Huanquan Pan, who gave guidance and support during the whole process. His initial idea formed the basis of this work.

I thank Dr. Dennis Voskov and Yaqing Fan for insightful discussions related to the project. They were always patient and warm-hearted. Thanks also to Hui Zhou for helping me with my thesis. Thanks to the SUPRI-B group and the Department of Energy Resources Engineering at Stanford for providing me with the financial means to complete this work. Thanks to all the other group members and faculty who had ever helped me. The attention and support that all of you have shown to me have been an encouragement to my work.

Thanks to my parents who endured this long process with me, and always offered support and love. And finally, thanks to my wife Jing for being incredibly understanding, supportive and patient.

# Contents

<b>Abstract</b>	<b>iii</b>
<b>Acknowledgements</b>	<b>iv</b>
<b>Table of Contents</b>	<b>v</b>
<b>List of Tables</b>	<b>vi</b>
<b>List of Figures</b>	<b>vii</b>
<b>1 Introduction</b>	<b>1</b>
1.1 Fluid Models . . . . .	2
1.1.1 Black-Oil Model . . . . .	2
1.1.2 Compositional Model . . . . .	3
1.2 Variable Bubble Point Problems . . . . .	5
<b>2 Two Pseudo-Component Approach</b>	<b>13</b>
2.1 Variable Switching Strategy in TPCA . . . . .	14
2.2 Equations and Variables . . . . .	15
2.3 TPCA Fluid Properties . . . . .	16
2.4 Black-Oil Flash . . . . .	18
2.5 TPCA Implementation in GPRS . . . . .	19
<b>3 Case Studies</b>	<b>27</b>
3.1 Case Descriptions . . . . .	27

3.2	Case 1: Depletion Case . . . . .	29
3.3	Case 2: Water Injection . . . . .	29
3.4	Case 3: Gas Injection . . . . .	32
3.5	Case 4: Alternate Water and Gas Injection . . . . .	35
<b>4</b>	<b>Conclusions and Future Work</b>	<b>45</b>

# List of Tables

1.1	Sample of black-oil PVT table . . . . .	3
1.2	Summary of the functional relationships for fluid properties . . . . .	11
2.1	Variable switching strategy in TPCA . . . . .	15
3.1	Data and constraints . . . . .	28
3.2	Grid description . . . . .	28
3.3	Case1: Initial distribution of $R_g$ and bubble-point pressure . . . . .	29

# List of Figures

1.1	Formulation level view of GPRS [2] . . . . .	5
1.2	Bubble point in the PVT data . . . . .	7
1.3	Bubble point and GOR vary with depth . . . . .	9
1.4	Bubble point decreasing case . . . . .	10
1.5	Bubble point increasing case . . . . .	10
2.1	Black-oil flash flowchart . . . . .	20
2.2	Extrapolations on PVT data . . . . .	21
2.3	Constant compressibility of undersaturated oil . . . . .	22
2.4	Bubble point pressure as a function of $z_o$ . . . . .	23
2.5	Flowchart of TPCA . . . . .	24
2.6	Data structure of fluid and phase with TPCA model in GPRS . . . . .	25
2.7	Update of structure in GPRS . . . . .	26
3.1	Reservoir and grid system . . . . .	28
3.2	Oil and gas production rates [Case 1] . . . . .	30
3.3	$p$ and $S_g$ in production block (1,1,1) [Case 1] . . . . .	31
3.4	Oil and gas production rates [Case 2] . . . . .	33
3.5	$p$ and $S_g$ at producer block (1,1,1) [Case 2] . . . . .	34
3.6	Water injection rate [Case 2] . . . . .	35
3.7	$p$ and $S_g$ at injector block (10,10,3) [Case 2] . . . . .	36
3.8	Oil and gas production rates [Case 3] . . . . .	37
3.9	$p$ and $S_g$ at producer block (1,1,1) [Case 3] . . . . .	38
3.10	Gas injection rate [Case 3] . . . . .	39



3.11 $p$ and $S_g$ at injector block (10,10,3) [Case 3] . . . . .	40
3.12 Oil and gas production rates [Case 4] . . . . .	41
3.13 $p$ and $S_g$ at producer block (1,1,1) [Case 4] . . . . .	42
3.14 Gas and water injection rates [Case 4] . . . . .	43
3.15 $p$ and $S_g$ at injector block (10,10,3) [Case 4] . . . . .	44

# Chapter 1

## Introduction

In reservoir simulation, the fluid model describes the physical properties of the reservoir fluids, which depend on the pressure, temperature and composition. Two kinds of fluid models are widely used in reservoir simulation: black-oil and compositional. In the black-oil model, two pseudo components, namely, oil and gas, are used to describe the hydrocarbon fluid system. A third pseudo component is used to describe the water. The pseudo components are usually defined as phases at standard conditions. For example, the gas (vapor) and oil (liquid) at surface conditions are labeled as the gas and oil pseudo components, respectively. In the generalized black-oil formulation, each phase (gas, oil, or water) at reservoir conditions can be made up of two pseudo components. One can associate a component with a master phase. For example, it is natural to associate the gas pseudo component with the gas phase. In the standard black-oil model, only the gas component is allowed to dissolve in the oil phase. For a given reservoir temperature, The gas solubility is usually expressed as the gas-oil-ratio as a function of pressure. In addition to the solubility, the black-oil model employs the concept of formation volume factor, which is defined as the ratio of the fluid phase volume at reservoir conditions to that at standard conditions.

In essence, the black-oil approach employs a simple model to represent the PVT (pressure-volume-temperature) behavior of the reservoir fluids. The behavior of a fluid mixture depends strongly on the phase state of the system. For a given temperature, the point at which the hydrocarbon fluid mixture goes from a single-phase

liquid (made up of the oil pseudo component and dissolved gas pseudo component) to two phases, is called the bubble-point pressure. The General Purpose Research Simulator (GPRS) is based on the assumption of a fixed bubble point. This assumption precludes the ability to handle variable bubble point problems, which form an important class of problem that a black-oil simulator should be able to model correctly and efficiently. In this report, we implement a Two Pseudo Component Approach (TPCA) [5] that extend the capabilities of GPRS to variable bubble point problems. The TPCA module employs the compositional code branch in GPRS to perform the simulations, and the ultimate goal is to replace the standard black-oil code branch with this TPCA framework.

In this chapter, a brief review of the standard black-oil and compositional models is given along with a simple introduction to GPRS. Then, reservoir processes where the bubble point can change as a function of location and time are described.

## 1.1 Fluid Models

The black-oil and compositional models are the heart of this work. The basis of the two models are introduced below.

### 1.1.1 Black-Oil Model

In a reservoir, the crude oil and gas contain many hydrocarbon components. In the black-oil model, all the components are categorized into two classes: stock tank oil (i.e., liquid oil at the surface) and separator gas. Using a reservoir fluid sample, fluid properties, such as viscosity, formation volume factor, and solubility are measured in the laboratory and tabulated as a function of pressure and temperature. An example is given in Table 1.1. During a simulation run, given the pressure and temperature, which is usually fixed, the PVT table is used to look up the fluid property of interest.

If the water phase is included, the standard black-oil model has three phases and three (pseudo) components. The flow equations for the black-oil model are shown in

Table 1.1: Sample of black-oil PVT table

Pressure psi	$B_o$ RB/STB	Viscosity cp	$R_o$ SCF/STB
14.7	1.062	1.040	1.0
264.7	1.150	0.975	90.5
514.7	1.207	0.910	180.0
1014.7	1.295	0.830	371.0
2014.7	1.435	0.695	636.0
2514.7	1.500	0.641	775.0
3014.7	1.565	0.594	930.0
4014.7	1.695	0.510	1270.0
5014.7	1.671	0.549	1270.0

Eq. 1.1, 1.2 and 1.3,

$$\begin{aligned} & \frac{\partial}{\partial t} [V\phi(S_g\rho_g + S_o\frac{\rho_{gst}}{B_o}R_g)] - \sum_l [T(\lambda_g\rho_g\Delta\phi_g + \lambda_o\frac{\rho_{gst}}{B_o}R_g\Delta\phi_o)] \\ & + \sum_w [WI(\lambda_g\rho_g(p_g - p^w) + \lambda_o\frac{\rho_{gst}}{B_o}R_g(p_o - p^w))] = 0, \end{aligned} \quad (1.1)$$

$$\begin{aligned} & \frac{\partial}{\partial t} [V\phi(S_g\frac{\rho_{ost}}{B_g}R_o + S_o\rho_o)] - \sum_l [T(\lambda_g\frac{\rho_{ost}}{B_g}R_o\Delta\phi_g + \lambda_o\rho_o\Delta\phi_o)] \\ & + \sum_w [WI(\lambda_g\frac{\rho_{ost}}{B_g}R_o(p_g - p^w) + \lambda_o\rho_o(p_o - p^w))] = 0, \end{aligned} \quad (1.2)$$

$$\frac{\partial}{\partial t} (V\phi S_w\rho_w) - \sum_l (T\lambda_w\rho_w\Delta\phi_w) + \sum_w [WI\lambda_w\rho_w(p_w - p^w)] = 0. \quad (1.3)$$

Eq. 1.1 to Eq. 1.3 are primary equations, and they can be directly expressed as functions of three primary variables. In the standard black-oil model, the three primary variables are pressure and two saturations. In our case, we choose  $p$ ,  $S_g$  and  $S_o$ .

### 1.1.2 Compositional Model

In a compositional model, the number of components can be quite large, and the dependance of the PVT phase behavior on composition must be modeled. The general

compositional flow equations are shown in Eq. 1.4 ~ Eq. 1.8.

$$\begin{aligned} \frac{\partial}{\partial t}[V\phi(S_g\rho_g y_c + S_o\rho_o x_c)] - \sum_l [T(\lambda_g\rho_g y_c \Delta\phi_g + \lambda_o\rho_o x_c \Delta\phi_o)] \\ + \sum_W [WI(\lambda_g\rho_g y_c(p_g - p^w) + \lambda_o\rho_o x_c(p_o - p^w))] = 0, \end{aligned} \quad (1.4)$$

$$c = 1, \dots, n_h,$$

$$\frac{\partial}{\partial t}(V\phi S_w \rho_w) - \sum_l (T\lambda_w \rho_w \Delta\phi_w) + \sum_W [WI\lambda_w \rho_w (p_w - p^w)] = 0, \quad (1.5)$$

$$f_c^v - f_c^l = 0, \quad (1.6)$$

$$\sum_c y_c = 1, \quad (1.7)$$

$$\sum_c x_c = 1, \quad (1.8)$$

where  $c = 1, \dots, n_h$ .  $f_c^v$  and  $f_c^l$  are the fugacities of component  $c$  in the gas and liquid phases, respectively. Similarly,  $y_c$  and  $x_c$  are the compositions of component  $c$  in the gas and liquid phases. The number of hydrocarbon components is  $n_h$ .

The variable set in the formulation can be divided into primary and secondary sets as follows:

Primary variables:  $p_g, S_g, S_o, y_c, c = 1, \dots, n_h - 2,$

Secondary variables:  $y_{n_h-1}, y_{n_h}, x_c, c = 1, \dots, n_h.$

Eq. 1.4 and Eq. 1.5 comprise  $n_h + 1$  equations, which are primary equations corresponding to  $n_h + 1$  primary variables. Eq. 1.6 to Eq. 1.8 comprise  $n_h + 2$  secondary equations.

An equation-of-state (EOS) model is usually used to describe the phase equilibrium behavior (secondary equations). These EOS computations include hydrocarbon phase-state identification (i.e., single-phase gas, single-phase oil, oil and gas), and when necessary, flash computations to determine the phase compositions. In the flash calculations, detailed information regarding the specific multi-component EOS model and its parameters are needed. In compositional simulations, the EOS computations can consume the bulk of the computations.

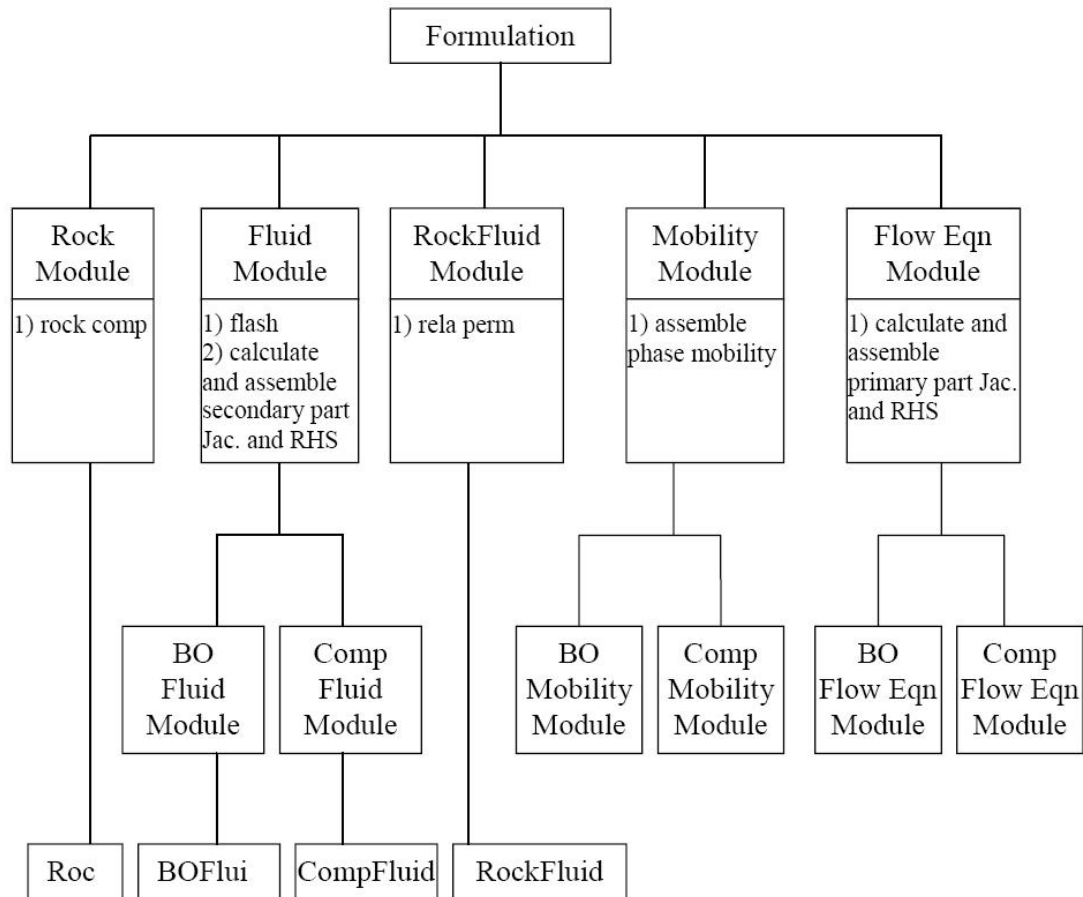


Figure 1.1: Formulation level view of GPRS [2]

## 1.2 Variable Bubble Point Problems

GPRS (General Purpose Research Simulator) is an in-house research simulator initially built by Cao [2]. Since then, GPRS has become a general and computationally efficient research platform. Numerous new research ideas from the Reservoir Simulation Group of Stanford University Petroleum Research Institute (SUPRI-B) have been integrated into GPRS. The basic structure of GPRS is shown in Fig. 1.1. As Fig 1.1 indicates, the black-oil and compositional models have been implemented using independent modules. The black-oil model assumes that the bubble-point pressure is fixed, and our objective is to remove this restriction.

In the black-oil model, the PVT table is obtained from experiments using a reservoir fluid sample. The experiments normally start at a high pressure such that the fluid is undersaturated (i.e., single-phase liquid). As the pressure is reduced, the liquid, which contains oil and gas, expands. With the decrease in pressure, the first bubble of gas appears, and we have two phases. The bubble point pressure  $p_b$  is the pressure at which this first bubble of gas appears. The fluid properties change dramatically when the phase state changes.

In the sample shown in Table 1.1, the bubble point pressure is 4014.7 psi.  $B_o$  and  $R_g$  are plotted in Fig. 1.2 as functions of pressure. Significant changes are observed in the properties as we go through the bubble point pressure. Let us examine the behavior of  $B_o$ , which denotes the oil formation volume factor of in reservoir barrels per stock-tank barrel (RB/STB). Below the bubble point, as the pressure increases, the oil volume increases because more gas is dissolved in it, and  $B_o$  keeps on increasing. When the pressure is above the bubble point pressure, no free gas is present since all the gas is dissolved in the oil (liquid). In this case, the volume of the liquid phase decreases with pressure. So,  $B_o$  decreases.

In GPRS, it is assumed that unique  $R_g$  and  $B_o$  curves are defined, and the bubble point is fixed. The fixed bubble-point treatment works well for pure depletion cases. Consider a depletion process of an initially saturated reservoir, i.e., the initial reservoir pressure is lower than the bubble point pressure so that we have two hydrocarbon phases. During a depletion process, where at any point in time and space, the reservoir pressure is either the same or is decreasing, the reservoir is always in the two-phase region. In this case, the table with a fixed bubble-point provides an accurate description of the PVT behavior.

However, there are several instances when this assumption is not valid because the bubble point pressure is not constant. The bubble point depends on the composition of the fluid, which can be represented by the gas-oil ratio in the black-oil model. All the gas can dissolve in the oil only if the pressure is high enough, which means that the bubble point pressure increases with increasing gas solubility. In a reservoir, when the thickness of the reservoir is large, the gas solubility may change with depth. So in some cases, the variation of the bubble point with depth cannot be ignored. This

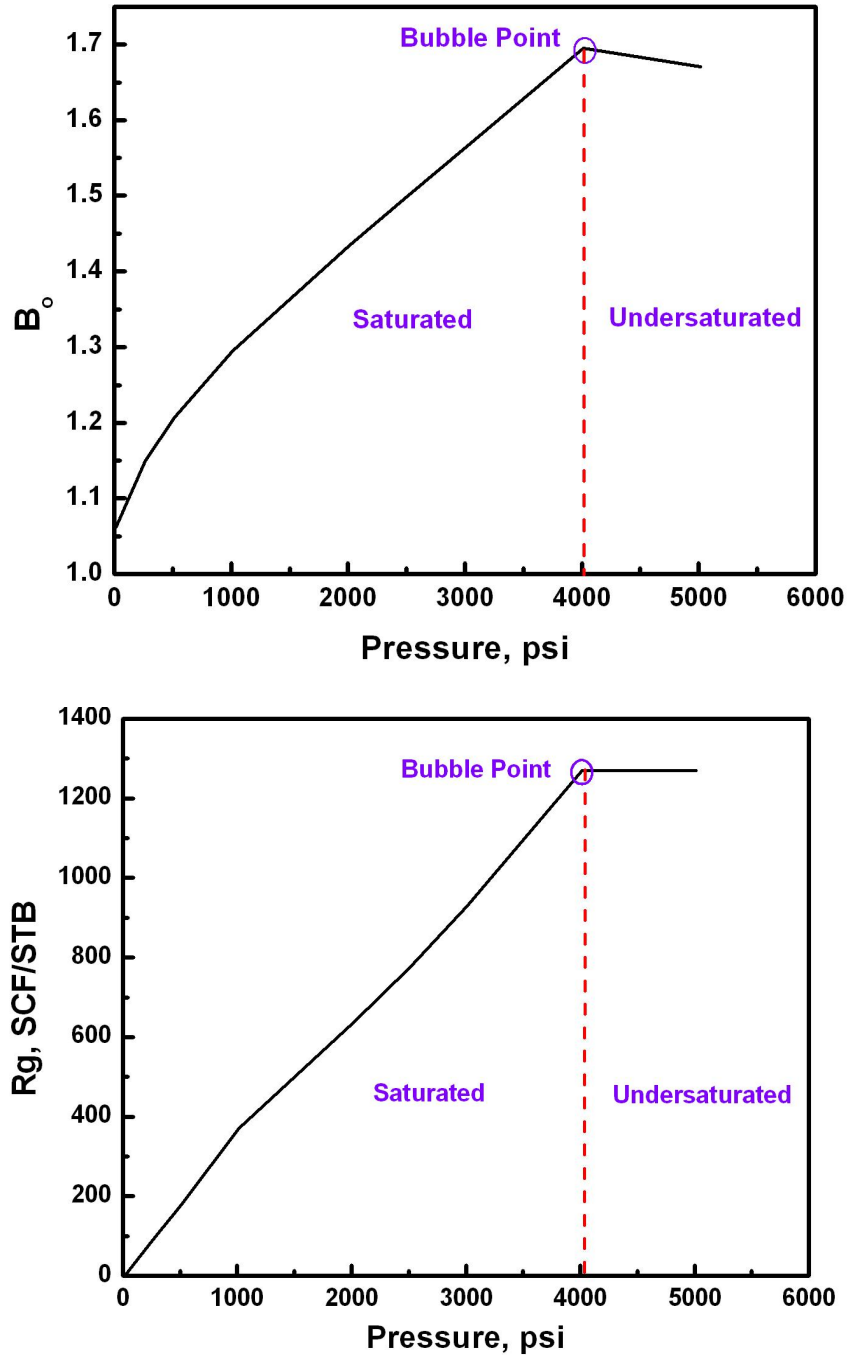


Figure 1.2: Bubble point in the PVT data



is illustrated in Fig. 1.3.

At a particular location in the reservoir, the bubble point may change with time. Consider one block in a reservoir with initial conditions given by point A in Fig. 1.4. The block is initially occupied by undersaturated oil (single-phase liquid). The initial pressure is  $P_1$ , and the bubble point pressure is  $P_{b1}$ . If the pressure is reduced to  $P_{b1}$ , the first gas bubble evolves at point B, and the oil is saturated. If the pressure decreases further, more free gas is released from the saturated oil. If when point C is reached, where the pressure is  $P_{b2}$ , all the free gas is removed (e.g., flows out of the gridblock due to its large mobility) the block becomes fully occupied by the (liquid) oil phase. The oil becomes undersaturated again. Suppose the block pressure is then increased to  $P_1$  due to water injection, the C→D path will be followed rather than the C→B→A path. The pressure is back to  $P_1$ , but we have a new bubble point,  $P_{b2}$ .

Fig. 1.5 shows a different setting. Suppose that at point B, gas is injected into the block and the pressure increases, the swelling curve to point E with the pressure  $P_{b3}$  is followed. At point E, all the injected gas is dissolved into the oil, and the oil becomes undersaturated. If the pressure increases to  $P_1$  and reaches point F, the new bubble point is  $P_{b3}$ .

As described above, in one reservoir simulation, although both the initial conditions and the current gridblock pressure are the same, the bubble-point may vary because of changes in the gas-oil ratio during the history of the flow process. Various methods have been proposed to handle variable bubble point problems.

Steffensen and Sheffield [3] and Kazemi [4] presented a method where the bubble point was treated as a variable in the accumulation terms only. When the pressure is lower than the bubble point pressure,  $B_o$  and  $R_g$  are functions of pressure only. However, when pressure is higher than the bubble-point pressure,  $B_o$  and  $R_g$  are functions of both pressure and bubble-point pressure. The functional relationships are listed in Table 1.2.

When pressure is higher than the bubble point pressure, there is no free gas, i.e.,  $S_g$  is zero. So, for a gridblock with no gas phase,  $S_g$  cannot be used as a primary variable in a standard black-oil implementation (or a compositional formulation based

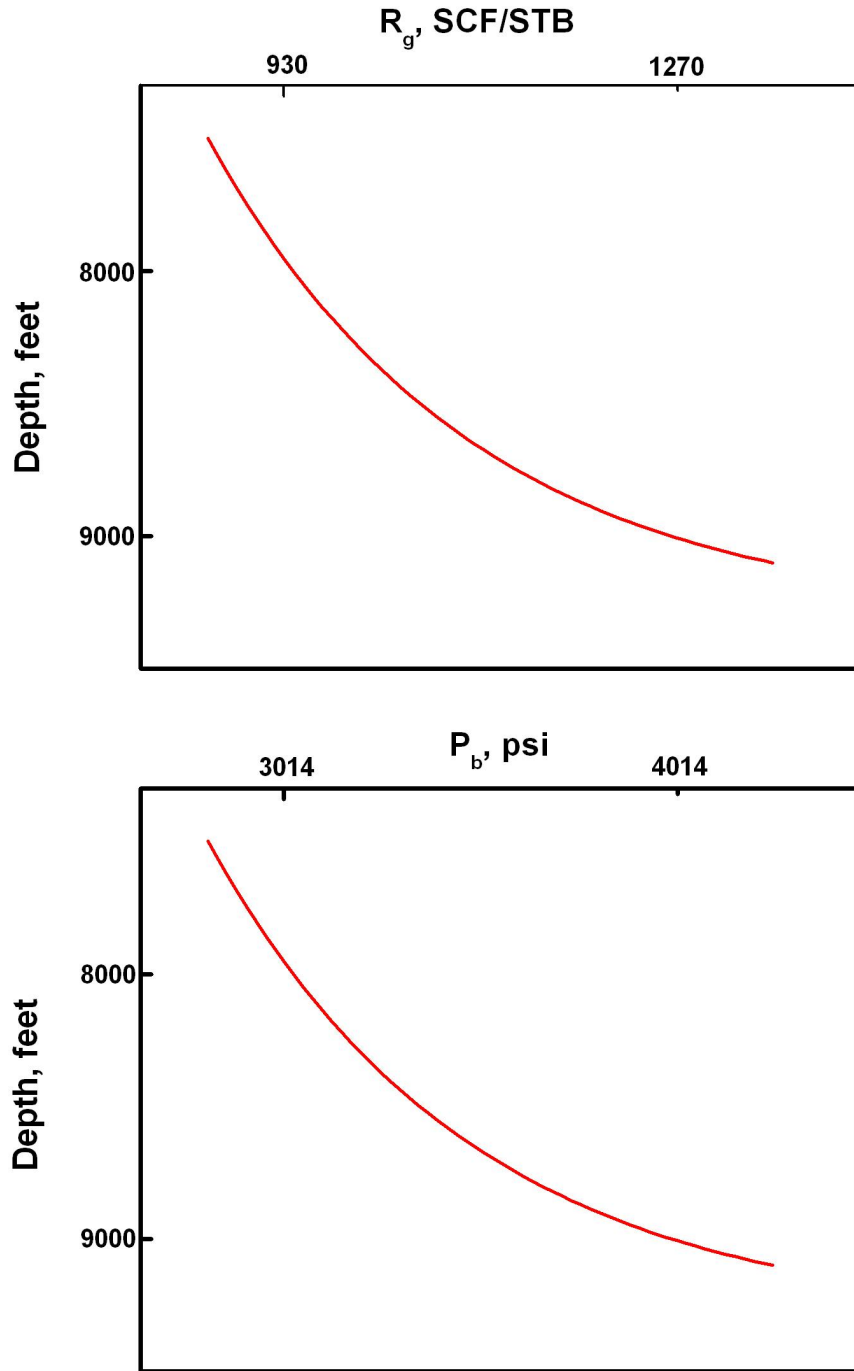


Figure 1.3: Bubble point and GOR vary with depth

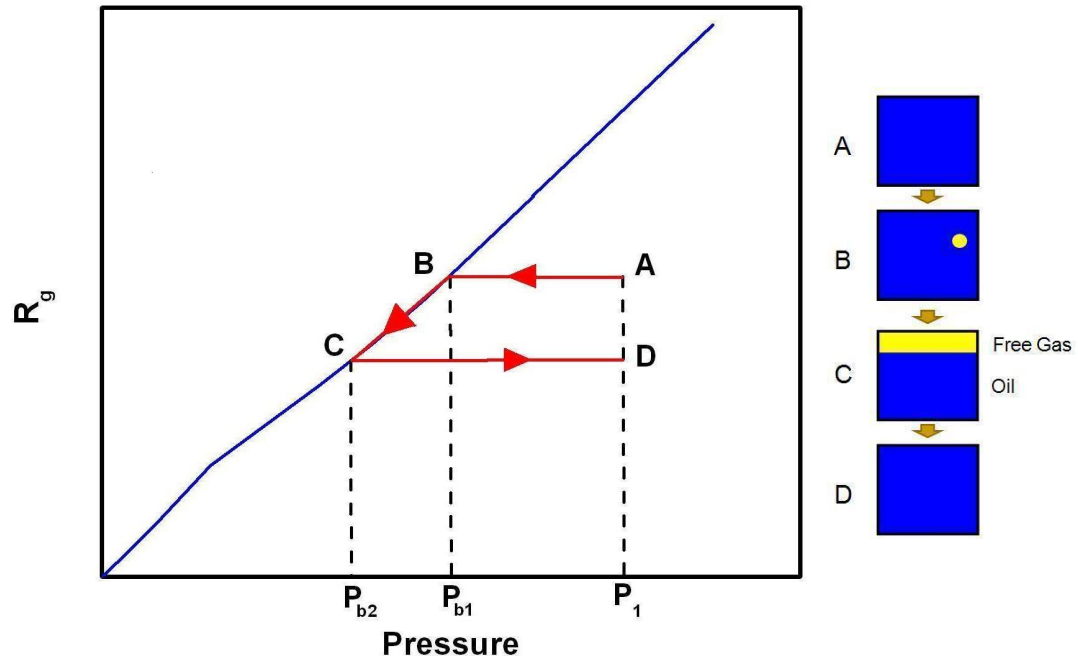


Figure 1.4: Bubble point decreasing case

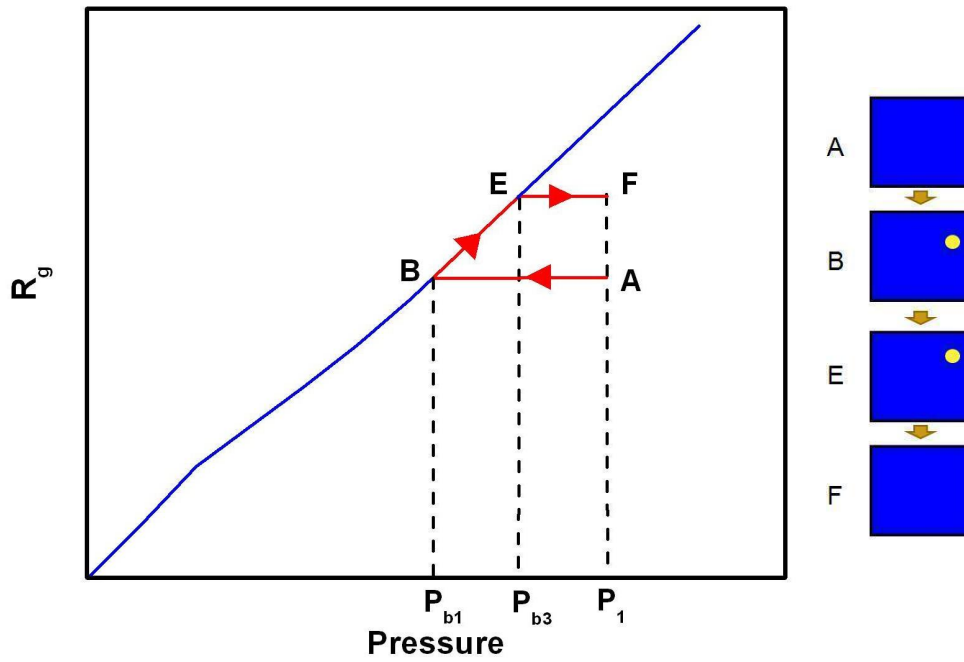


Figure 1.5: Bubble point increasing case

Table 1.2: Summary of the functional relationships for fluid properties

Property	Saturated Oil	Undersaturated Oil
$B_o$	$B_o(p)$	$B_o(p, p_{bp})$
$\mu_o$	$\mu_o(p)$	$\mu_o(p, p_{bp})$
$R_g$	$R_g(p)$	$R_g(p, p_{bp})$

on the natural variable set). In this case, variable substitution is necessary. There are several possible candidates for the variable switching strategy. In the ECLIPSE 100 simulator, the new variable is  $R_g$ . So when the gas phase disappears, the independent variable set becomes  $p, S_w, R_g$ . The black-oil module in GPRS does not employ variable switching, and  $p, S_g$  and  $S_o$  are always used as primary variables. This prevents us from simulating variable bubble-point problems using the black-oil module.

On the other hand, the compositional model in GPRS has a natural variable implementation with a robust variable switching strategy for phase appearance (disappearance/reappearance). For example, when gas disappears, a composition variable is used as a primary variable to take the place of  $S_g$ . So one can always use the fully compositional treatment in GPRS to model variable bubble-point problems. In the next chapter, we describe the implementation of a two pseudo-component approach [5] to deal with problems where the bubble point pressure changes in different parts of the reservoir as a function of time. This approach is intended to replace the black-oil code branch in GPRS.



## Chapter 2

# Two Pseudo-Component Approach

As mentioned in Chapter 1, variable bubble point problems are related to phase-state changes. The compositional routine in GPRS can handle phase appearance and disappearance effectively, so it is natural to use a compositional approach to solve variable bubble point problems.

Shank and Vestal [5] presented an elegant Two Pseudo Component Approach (TPCA) for modeling black-oil problems. In this approach, there are two pseudo-components: stock tank oil and separator gas. So, the hydrocarbon fluid in the standard black-oil model is treated rigorously as a two pseudo-component compositional formulation that uses a simple representation of the phase behavior (e.g., pressure dependent solubility and formation-volume factors).

This two-component representation meets the following requirements:

1. Models variable bubble point problems.
2. Accepts Standard black-oil input, which means that no more additional information is required to the TPCA model.
3. Uses the existing compositional code branch in GPRS.
4. Yields computational efficiency that is comparable to the black-oil model.

Next, we describe how to translate the black-oil model into a compositional form.

Then, the expressions of the TPCA fluid properties are given. Finally, the method used to implement the TPCA model into GPRS is described.

## 2.1 Variable Switching Strategy in TPCA

In a compositional model with two hydrocarbon (pseudo) components, one choice for the variable sets is given by:

Primary variables:  $p, S_g, S_o,$

Secondary variables:  $y_g, y_o, x_g, x_o.$

The TPCA model uses this description. Here,  $y_g$  and  $x_g$  are gas compositions in the gas and liquid phases, respectively. Similarly,  $y_o$  and  $x_o$  are the oil compositions.

The phase compositions can be explicitly computed using the following expressions:

$$y_g = \frac{1}{1 + r_o}, \quad (2.1)$$

$$y_o = \frac{r_o}{1 + r_o}, \quad (2.2)$$

$$x_g = \frac{r_g}{1 + r_g}, \quad (2.3)$$

$$x_o = \frac{1}{1 + r_g}, \quad (2.4)$$

where,  $r_g$  is the solution gas-oil-ratio on molar basis, and  $r_o$  is the vaporized oil-gas-ratio on molar basis. They can be derived from solubility data,  $R_g$  and  $R_o$ , using Eq. 2.5 and Eq. 2.6,

$$r_g = R_g \frac{\bar{\rho}_{gst}}{\bar{\rho}_{ost}}, \quad (2.5)$$

$$r_o = R_o \frac{\bar{\rho}_{ost}}{\bar{\rho}_{gst}}, \quad (2.6)$$

where  $\bar{\rho}_{gst}$  and  $\bar{\rho}_{ost}$  are the gas and oil molar densities at standard conditions. Based on the Eq. 2.1 to Eq. 2.6, the solubility data  $R_g$  and  $R_o$  are translated into phase compositions, namely,  $y_g, y_o, x_g$  and  $x_o$ .

Table 2.1: Variable switching strategy in TPCA

Phase state	Primary variable set
Gas and Oil	$p, S_g, S_o$
Oil only	$p, S_o, x_g$
Gas only	$p, S_g, y_g$

When phases disappear or reappear, the TPCA model follows the variable switching strategy of the compositional module in GPRS. The variable switching strategy is given in Table 2.1.

## 2.2 Equations and Variables

The black-oil model is a simplified compositional model with only two components. So the primary equations of black-oil model (Eq. 1.1 and Eq. 1.2) can be written as Eq. 2.7 and Eq. 2.8:

$$\begin{aligned} & \frac{\partial}{\partial t} [V\phi(S_g\rho_g y_c + S_o\rho_o x_c)] - \sum_l [T(\lambda_g\rho_g y_c \Delta\phi_g + \lambda_o\rho_o x_c \Delta\phi_o)] \\ & + \sum_w [WI(\lambda_g\rho_g y_c (p_g - p^w) + \lambda_o\rho_o x_c (p_o - p^w))] = 0, \end{aligned} \quad (2.7)$$

$c = g, o,$

$$\frac{\partial}{\partial t} (V\phi S_w \rho_w) - \sum_l (T\lambda_w \rho_w \Delta\phi_w) + \sum_w [WI\lambda_w \rho_w (p_w - p^w)] = 0. \quad (2.8)$$

The secondary equations should provide the constraints to build relations between secondary variables and primary variables. According to Aziz and Settari [1], the equilibrium ratios, or K-values can be calculated as follows:

$$K_g = \frac{y_g}{x_g}, \quad (2.9)$$

$$K_o = \frac{y_o}{x_o}. \quad (2.10)$$



Eq. 2.9 and Eq. 2.10 can be rewritten as:

$$y_g p - K_g x_g p = 0, \quad (2.11)$$

$$y_o p - K_o x_o p = 0. \quad (2.12)$$

Also we have:

$$y_g + y_o = 1, \quad (2.13)$$

$$x_g + x_o = 1. \quad (2.14)$$

Eq. 2.11 to Eq. 2.14 are used as secondary equations. Compare Eq. 2.11 and Eq. 2.12 with Eq. 1.6, we can define the black-oil fugacity as follows:

$$f_g^v = y_g p, \quad (2.15)$$

$$f_g^l = K_g x_g p, \quad (2.16)$$

$$f_o^v = y_o p, \quad (2.17)$$

$$f_o^l = K_o x_o p. \quad (2.18)$$

Because  $y_g$ ,  $x_g$ ,  $y_o$  and  $x_o$  are calculated from  $r_g$  and  $r_o$ , the K-values can be directly expressed as functions of  $r_g$  and  $r_o$ :

$$K_g = \frac{y_g}{x_g} = \frac{1 + 1/r_g}{1 + r_o}, \quad (2.19)$$

$$K_o = \frac{y_o}{x_o} = \frac{1 + r_g}{1 + 1/r_o}. \quad (2.20)$$

The derivatives of the K-values with respect to  $p$  are given by:

$$\frac{dK_g}{dp} = \frac{-\frac{1+r_o}{r_g^2} \frac{dr_g}{dp} - (1 + \frac{1}{r_g}) \frac{dr_o}{dp}}{(1 + r_o)^2}, \quad (2.21)$$

$$\frac{dK_o}{dp} = \frac{\frac{1+r_g}{r_o^2} \frac{dr_o}{dp} + (1 + \frac{1}{r_o}) \frac{dr_g}{dp}}{(1 + \frac{1}{r_o})^2}. \quad (2.22)$$

## 2.3 TPCA Fluid Properties

In GPRS, Newton's method is used to solve the nonlinear algebraic system of equations. In the Newton method, all the terms in the primary and secondary equations

should be derived with respect to the variable set. Since the derivatives with respect to saturation will be exactly the same as those in black-oil model, only the derivatives of fluid properties with respect to  $p$ ,  $y_c$ , and  $x_c$  are presented here.

In the compositional model of GPRS, the densities in the primary equations are defined as molar densities with the unit of lbm mol/ft<sup>3</sup>, so it is necessary to translate mass densities  $\rho_g$  and  $\rho_o$  into molar densities  $\bar{\rho}_g$  and  $\bar{\rho}_o$ . We have

$$\bar{\rho}_g = \frac{\rho_g}{M_{pg}} = \frac{\rho_g}{M_g y_g + M_o y_o}, \quad (2.23)$$

$$\bar{\rho}_o = \frac{\rho_o}{M_{po}} = \frac{\rho_o}{M_g x_g + M_o x_o}, \quad (2.24)$$

where  $M_g$  and  $M_o$  are the molecular weights of the gas and oil components, which are assumed to be constant.  $M_{pg}$  and  $M_{po}$  are the gas and oil phase molecular weights, which change with different compositions. Then, the density derivatives can be written as follows:

$$\frac{d\bar{\rho}_g}{dp} = \frac{\frac{d\rho_g}{dp}}{M_g y_g + M_o y_o}, \quad (2.25)$$

$$\frac{d\bar{\rho}_o}{dp} = \frac{\frac{d\rho_o}{dp}}{M_g x_g + M_o x_o}, \quad (2.26)$$

$$\frac{d\bar{\rho}_g}{dy_g} = -\frac{\rho_g M_g}{M_{pg}^2}, \quad (2.27)$$

$$\frac{d\bar{\rho}_g}{dy_o} = -\frac{\rho_g M_o}{M_{pg}^2}, \quad (2.28)$$

$$\frac{d\bar{\rho}_o}{dx_g} = -\frac{\rho_o M_g}{M_{po}^2}, \quad (2.29)$$

$$\frac{d\bar{\rho}_o}{dx_o} = -\frac{\rho_o M_o}{M_{po}^2}. \quad (2.30)$$

$y_g$ ,  $y_o$ ,  $x_g$  and  $x_o$  are regarded as independent variables here, and the relationships among them are shown in Eq. 2.13 and Eq. 2.14. The mass densities  $\rho_g$  and  $\rho_o$  are calculated from:

$$\rho_g = (\rho_{gst} + R_o \rho_{ost}) b_{wg}, \quad b_{wg} = b_g (1 + r_o), \quad (2.31)$$

$$\rho_o = (\rho_{ost} + R_g \rho_{gst}) b_o, \quad (2.32)$$

where  $b_g$  and  $b_o$  are the reciprocals of the gas and oil formation volume factors  $B_g$  and  $B_o$ , respectively.  $b_{wg}$  is the reciprocal of the wet gas formation volume factor  $B_{wg}$ . If there is dry gas,  $r_o = 0$  and  $b_{wg} = b_g$ . And the derivatives of the mass densities with respect to pressure are:

$$\frac{d\rho_g}{dp} = \rho_{ost} b_{wg} \frac{dR_o}{dp} + \frac{\rho_g}{b_{wg}} \frac{db_{wg}}{dp}, \quad (2.33)$$

$$\frac{d\rho_o}{dp} = \rho_{gst} b_o \frac{dR_g}{dp} + \frac{\rho_o}{b_o} \frac{db_o}{dp}. \quad (2.34)$$

Phase viscosities and their derivatives are exactly the same as those in the black-oil model. The derivatives with respect to  $y_g$ ,  $y_o$ ,  $x_g$ ,  $x_o$  are all equal to zero. In GPRS, these values in the compositional model are set to zero.

The fugacities and their derivatives were defined in Eq. 2.15 to Eq. 2.18. All the derivatives are given in Eqn. 2.35 to Eqn. 2.40:

$$\frac{df_g^l}{dp} = \left( \frac{dK_g}{dp} + K_g \right) x_g, \quad \frac{df_g^v}{dp} = y_g, \quad (2.35)$$

$$\frac{df_o^l}{dp} = \left( \frac{dK_o}{dp} + K_o \right) x_o, \quad \frac{df_o^v}{dp} = y_o, \quad (2.36)$$

$$\frac{df_g^l}{dx_g} = K_g p, \quad \frac{df_g^l}{dx_o} = 0, \quad (2.37)$$

$$\frac{df_g^v}{dy_g} = p, \quad \frac{df_g^v}{dy_o} = 0, \quad (2.38)$$

$$\frac{df_o^l}{dx_g} = 0, \quad \frac{df_o^l}{dx_o} = K_o p, \quad (2.39)$$

$$\frac{df_o^v}{dy_g} = 0, \quad \frac{df_o^v}{dy_o} = p. \quad (2.40)$$

## 2.4 Black-Oil Flash

The bubble point is the phase change point. So we can calculate the bubble point pressure according to the phase equilibrium rule given by

$$K_g z_g + K_o z_o = 1, \quad (2.41)$$

where  $z_g$  and  $z_o$  are the overall molar fractions of gas and oil and satisfy

$$z_g + z_o = 1. \quad (2.42)$$

K-values can be calculated from Eq. 2.19 and Eq. 2.20. Because the bubble point is in the two-phase region,  $r_g$  and  $r_o$  are functions of pressure only. K-values can be expressed as functions of  $r_g$  and  $r_o$ , so they are functions of pressure only. Therefore, if  $z_o$  is given, there is one corresponding pressure value satisfying Eq. 2.41; that value is the bubble point pressure.

As in standard flash calculations, the output of the black-oil flash is the phase state and the phase volume fraction.

- Step 1 Given  $p$  and  $z_o$ .  $R_g$  and  $R_o$  are obtained by table lookup.
- Step 2 Translate  $R_g$  and  $R_o$  into  $r_g$  and  $r_o$  using Eqs. 2.5 and 2.6.
- Step 3 Calculate K-values using Eqs. 2.19 and 2.20.
- Step 4 Check the phase state using Eq. 2.41; calculate molar fraction of gas phase,  $\bar{V}_g$ , from Eq. 2.43,

$$\bar{V}_g = \left( -\frac{z_g}{K_o - 1} - \frac{z_o}{K_g - 1} \right). \quad (2.43)$$

When the gas phase reappears,  $S_g$  can be obtained from  $\bar{V}_g$  using the following equation

$$S_g = \frac{1 - S_w}{1 + \left( \frac{1}{\bar{V}_g} - 1 \right) \frac{\rho_g}{\rho_o}}. \quad (2.44)$$

The flow chart for black-oil flash calculations is illustrated in Fig. 2.1.

## 2.5 TPCA Implementation in GPRS

We implemented a limited version of the TPCA framework in GPRS. The standard black-oil PVT table only provides the properties of the gas-oil system with a fixed gas-oil ratio. However, the TPCA model should describe the fluid properties of the gas-oil system with any gas-oil ratio. So, we make the following assumptions:

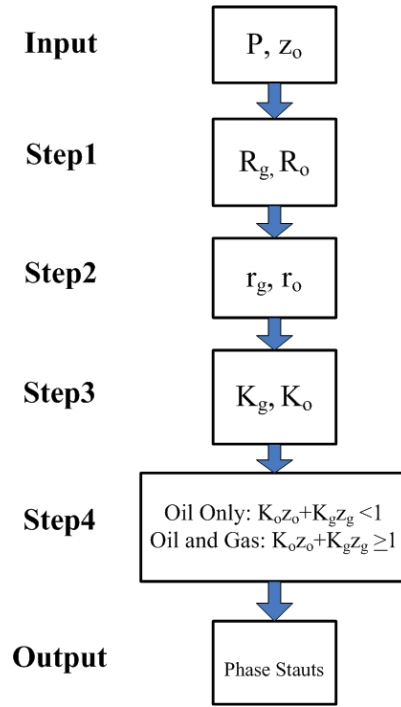


Figure 2.1: Black-oil flash flowchart

The input PVT table does not give the two-phase fluid properties information above the given bubble point. The only way to achieve this is by extrapolating the property curves in the PVT table. The extrapolations are based on the last two data points in the two-phase region. The extrapolations are illustrated in Fig. 2.2. Same extrapolation strategy is also applied to  $\mu_o$ , which is not presented here.

The input PVT table only provides the properties of undersaturated oil with a fixed gas-oil ratio. We should also make an assumption to describe the undersaturated oil with a different gas-oil ratio. In another words, different bubble points. The assumption is that the slope of the curves in the undersaturated oil region is constant. That is, we write

$$\frac{dB_o}{dp} = \text{constant for undersaturated oil} \quad (2.45)$$

$$\frac{d\mu_o}{dp} = \text{constant for undersaturated oil} \quad (2.46)$$

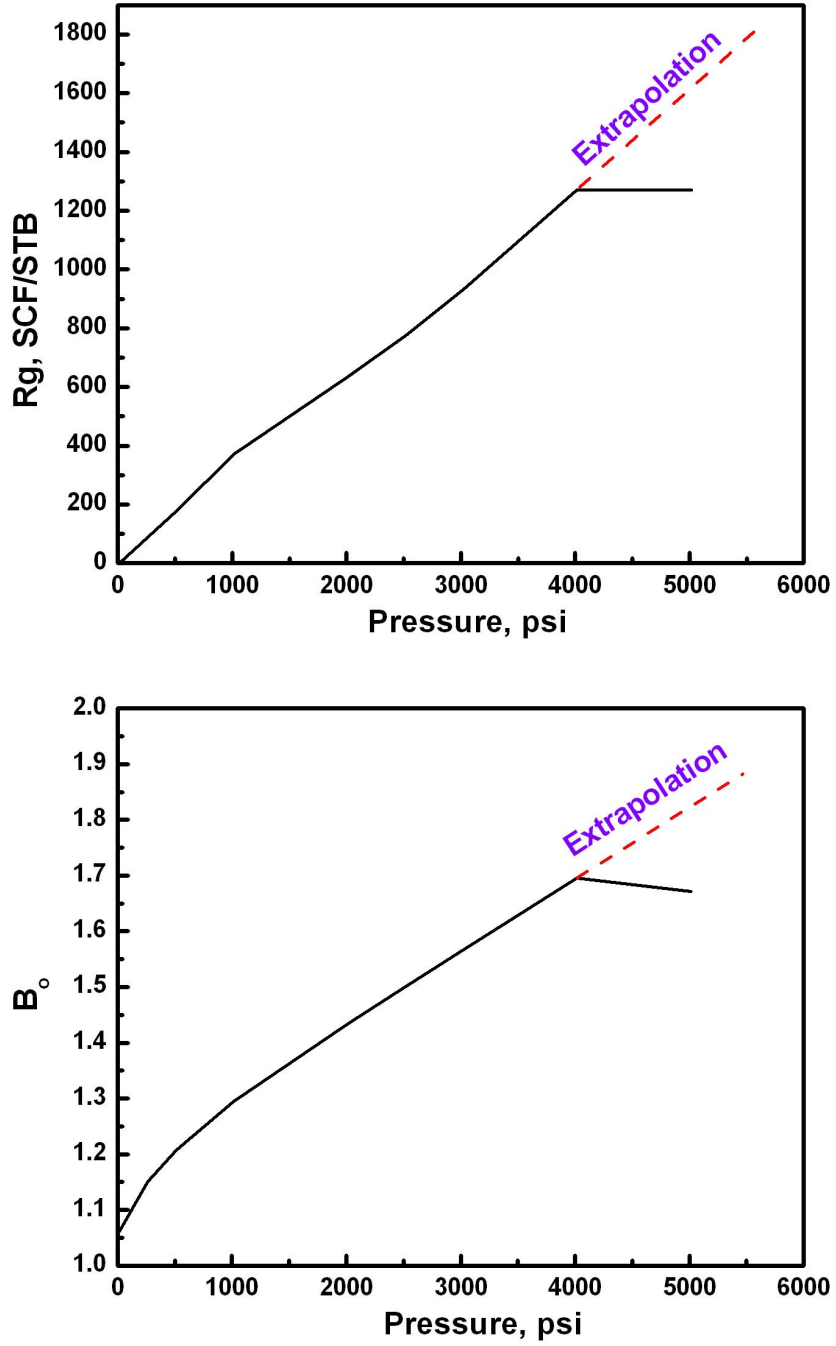


Figure 2.2: Extrapolations on PVT data

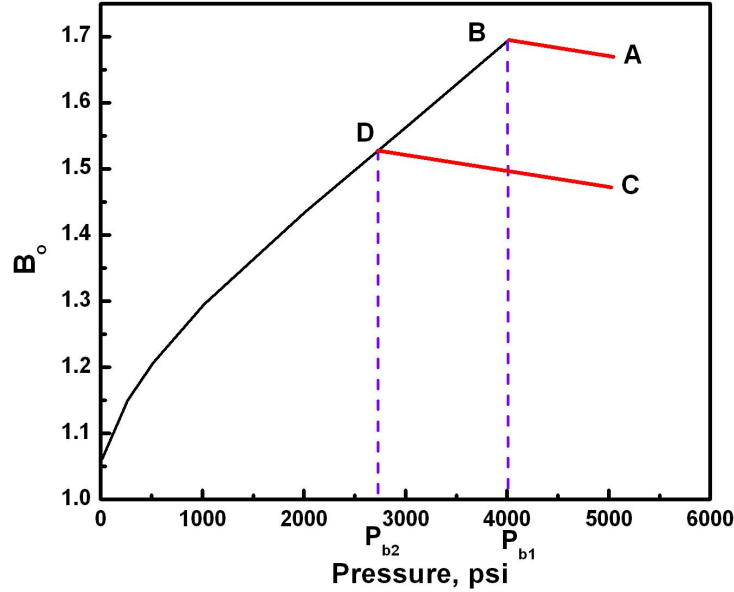


Figure 2.3: Constant compressibility of undersaturated oil

Illustrated in Fig. 2.3, AB designates  $B_o$  data above the bubble point pressure  $P_{b1}$ , and CD designates  $B_o$  data above the bubble point pressure  $P_{b2}$ . AB is parallel to CD, which means the compressibility is constant for different bubble points. This assumption is also adopted by the ECLIPSE 100 black-oil simulator [6].

In a standard black-oil input, the molecular weights of oil and gas are not provided. Molecular weight data are required by the compositional model only. Because TPCA is a compositional model and all the equations are built on molar basis, we assume that the molecular weights of gas and oil,  $M_g$  and  $M_o$  are given by

$$M_g = 23 \text{ lbm/lbm mol}, \quad M_o = 190 \text{ lbm/lbm mol}. \quad (2.47)$$

In fact, since all the terms in Eq. 2.7 are divided by the same molecular weight value, any non-zero values for the molar weights will work. The values in Eqn. 2.47 are just common values of the molecular weights for gas and oil.

The bubble-point pressure can be described as a function of  $z_o$ , and this relationship can be tabulated. In this bubble-point table, given  $z_o$ , we look up the

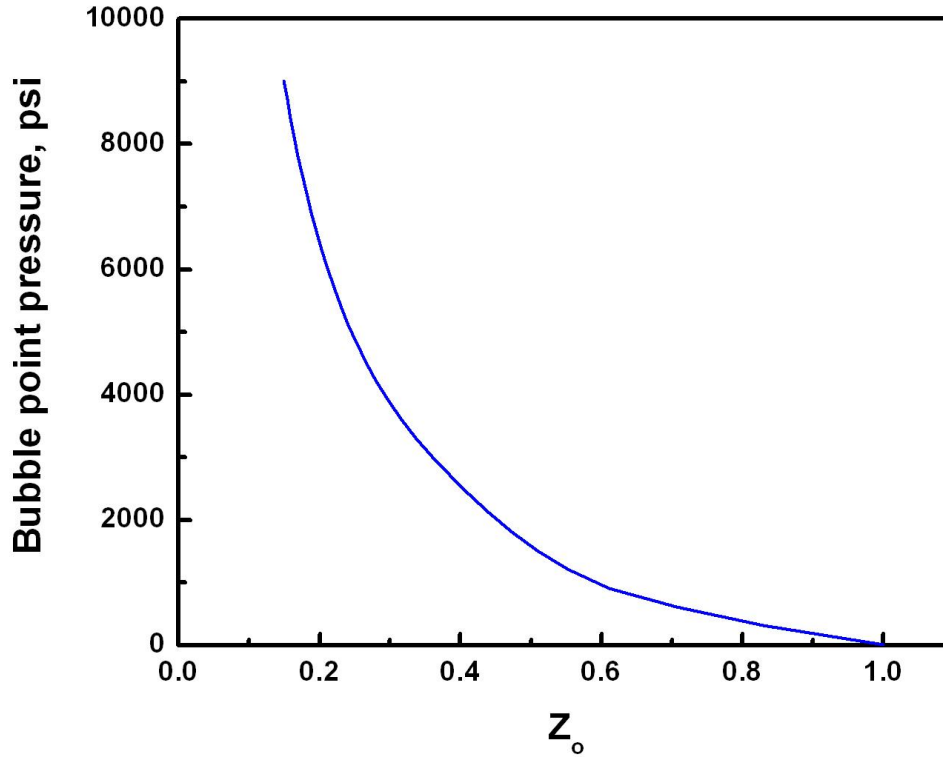


Figure 2.4: Bubble point pressure as a function of  $z_o$

corresponding bubble point pressure. During a simulation run, black-oil flash computations are obtained using table lookup, so the black-oil flash computations consume very little time. A preprocessing step is added to GPRS to generate the bubble point table. This procedure reads the PVT table and the bubble point pressure region. A set of  $z_o$  values and the corresponding bubble point pressures are then calculated and stored. An example bubble point curve is plotted in Fig. 2.4. As  $z_o$  increases,  $p_b$  decreases. This means when the overall oil fraction in a gas-oil system is larger, the bubble point pressure of the system is lower.

The TPCA implementation is shown in Fig. 2.5. First, a preprocessing step is used to generate the bubble point table based on the data in the standard PVT table. During a simulation run, black-oil flash calculations are carried out, and the



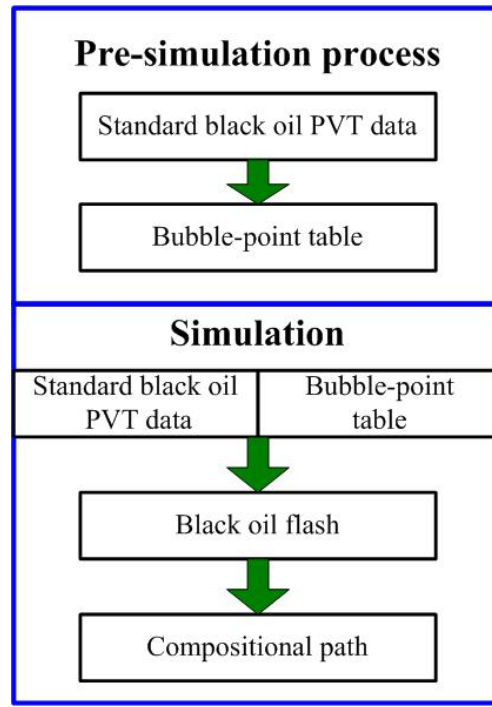


Figure 2.5: Flowchart of TPCA

phase state is determined. A new bubble point pressure is also calculated. With the new bubble point, the phase properties are obtained. This information is then used as input to the compositional module.

Two new classes are added to GPRS. The first is the *PVTCompFluid* class, which is derived from the *CompFluid* class, and it describes the TPCA fluid properties. The other is the *PVTPhase* class, which is derived from the *HCPPhase* class, and it describes the gas and oil phase properties in the TPCA model. The TPCA model is totally separated from the black-oil model, and is a subset of the compositional model. This means that TPCA can handle all the black-oil cases. The structure is shown in Fig 2.6. Fig 2.7 shows the updated flowchart of GPRS.

In next chapter, we will validate the TPCA model using several case studies.

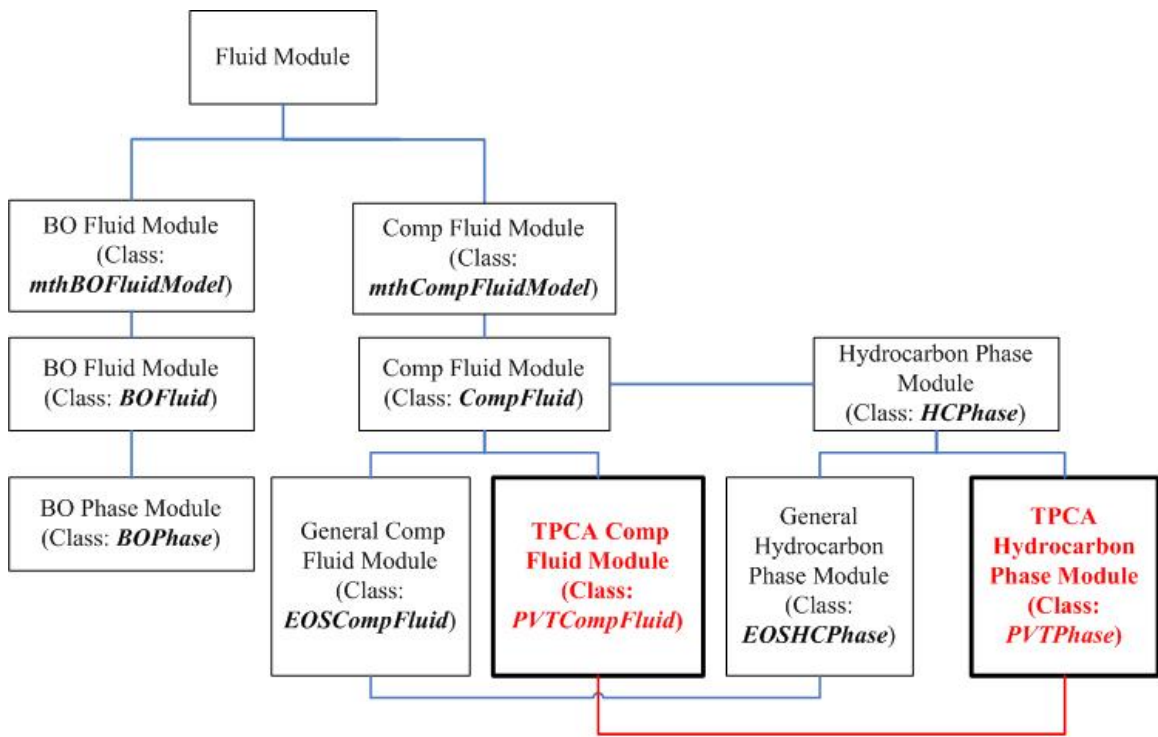


Figure 2.6: Data structure of fluid and phase with TPCA model in GPRS

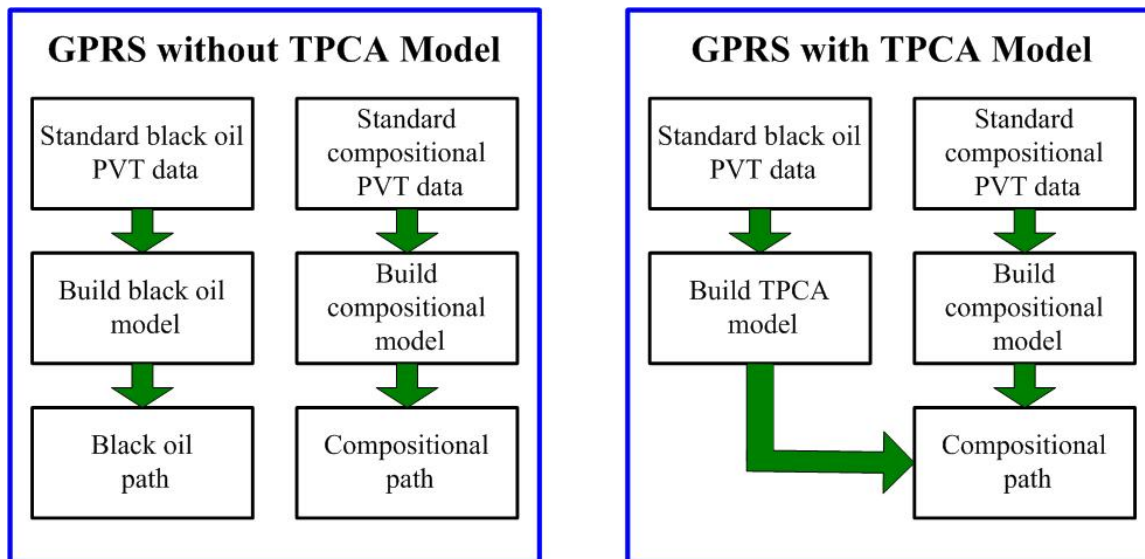


Figure 2.7: Update of structure in GPRS

# Chapter 3

## Case Studies

In this chapter, four cases are studied to validate the TPCA model. These problems test the TPCA implementation for accurate modeling of variable bubble point problems. First we introduce the initial conditions of these cases. Then the four cases are tested using both black-oil and TPCA models in GPRS. For the purpose of comparison, these cases are also simulated by the ECLIPSE 100 simulator.

### 3.1 Case Descriptions

The SPE 1 comparative solution problem [9] serves as a base case. Several cases modified from the SPE 1 problem are simulated using GPRS with the black-oil model, which assumes a fixed bubble point, and GPRS with TPCA.

All the four cases presented here share the same grid, rock properties, and PVT data. The reservoir model is initially occupied by undersaturated oil and connate water, which means the initial pressure is higher than the initial bubble point pressure. In Case 1, the initial bubble point is different in different layers. In Cases 2, 3 and 4, the initial bubble point is uniform in the whole reservoir. The reservoir conditions are described in Table 3.1, Table 3.2 and Fig. 3.1.

Table 3.1: Data and constraints

Options	Description
Initial Pressure	4020 psia at 8400 feet
Producer	BHP = 1000 psia
Injector	BHP = 8000 psia
Case 1	Injector is shut down
Case 2	Injecting water
Case 3	Injecting gas
Case 4	Alternate injection of gas and water

Table 3.2: Grid description

	$\phi$	$d_z$ , ft	$k_x$ , cp	$k_y$ , cp	$k_z$ , cp	$S_w$	$S_o$	Depth of center, ft
<b>LAYER 1</b>	0.3	20	500	500	50	0.16	0.84	8335
<b>LAYER 2</b>	0.3	30	50	50	25	0.16	0.84	8360
<b>LAYER 3</b>	0.3	50	200	200	25	0.16	0.84	8400

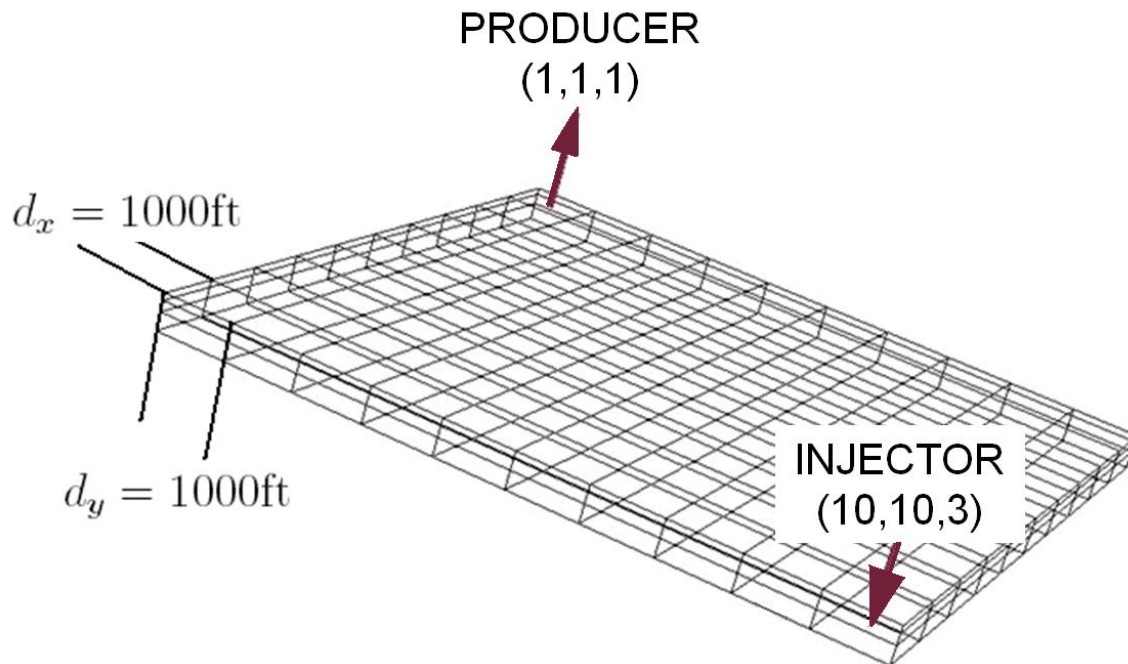


Figure 3.1: Reservoir and grid system

Table 3.3: Case1: Initial distribution of  $R_g$  and bubble-point pressure

	Depth, ft	$R_g$ , SCF/STB	$b_p$ , psi
Layer 1	8335	930	3014.6
Layer 2	8360	950	3076.6
Layer 3	8400	980	3166.7

## 3.2 Case 1: Depletion Case

In this case, we have a depletion problem with a single production well. The variable bubble point problem is due to the nonuniform initial distribution of  $R_g$ . The initial bubble point pressure increases with the depth, as shown in Table 3.3. In the GPRS black-oil model, it is always assumed that initial  $R_g$  is the same through the whole reservoir, so it cannot run this kind of problem. For the TPCA model, a ‘GOR Table’ is included in the input to define the initial distribution of  $R_g$ . With this table, we can set the initial  $R_g$  for each gridblock, and the corresponding initial bubble-point pressure,  $p_b$ , is computed.

Fig. 3.2 shows the production of oil and gas, and Fig. 3.3 illustrates the pressure and saturation histories in the production gridblock. The ECLIPSE 100 results are in good agreement with the TPCA GPRS simulations.

## 3.3 Case 2: Water Injection

In this case, water is injected for 7000 days. Consider the producer block (1,1,1). Due to the huge size of the reservoir, the pressure in the gridblock decreases early on because of depletion. When the block pressure is lower than the original bubble point pressure, gas is released from solution. Given the high pressure gradient, the free gas, which is much more mobile than the oil and water, flows out of the gridblock. As the pressure increases with water injection, no free gas is present, and the gridblock eventually becomes a single oil phase. The new bubble point pressure for this

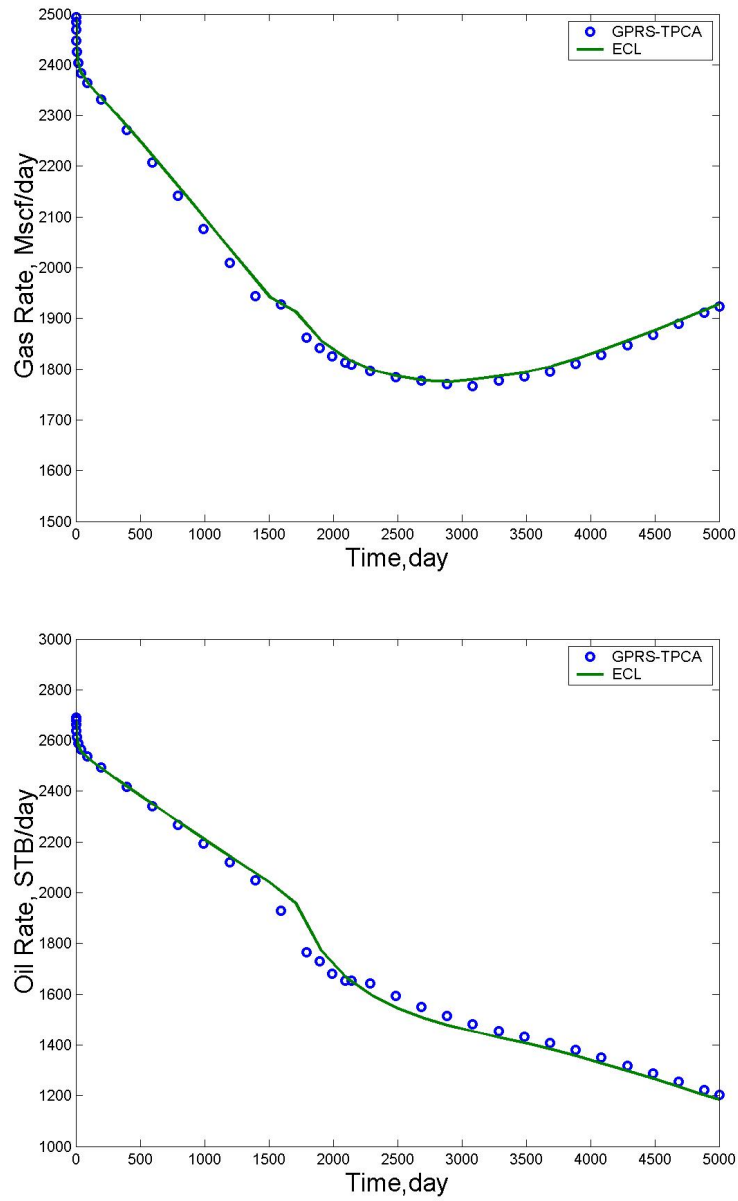


Figure 3.2: Oil and gas production rates [Case 1]

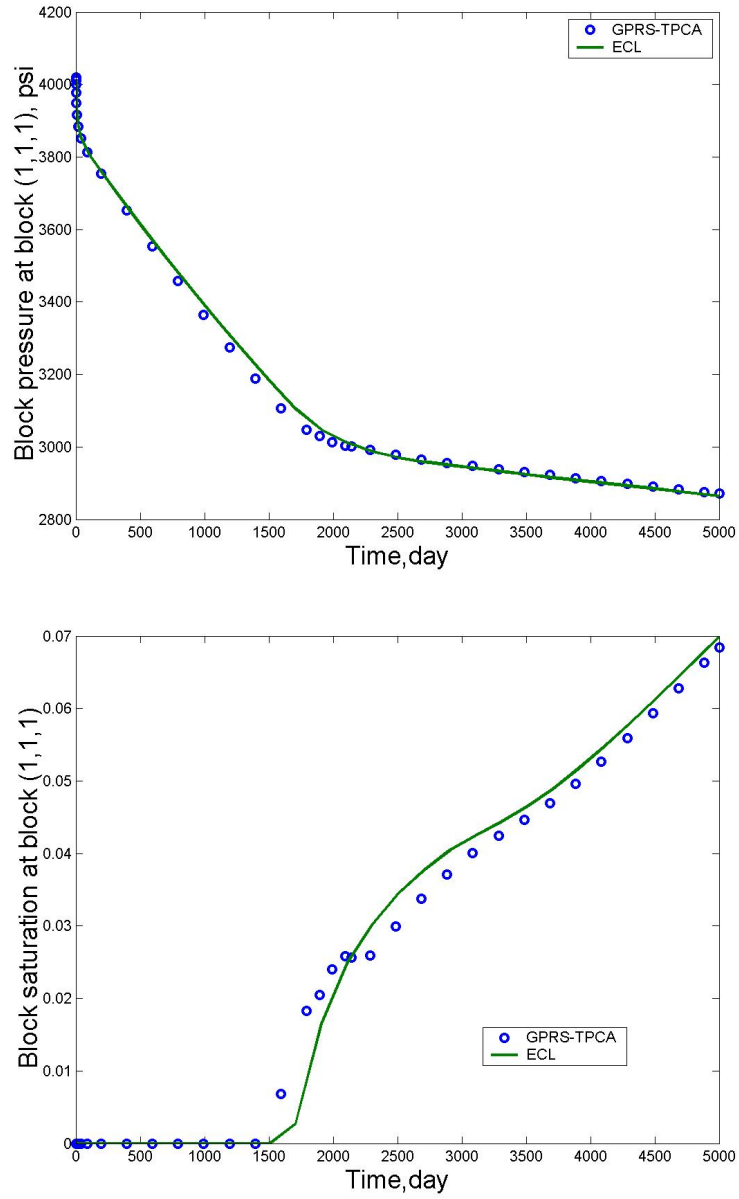


Figure 3.3:  $p$  and  $S_g$  in production block (1,1,1) [Case 1]



gridblock is the prevailing pressure. Accurate modeling of the appearance and disappearance of the gas phase is essential for accurate representation of the physics in this case. In Fig. 3.5, the saturation data show an obvious difference between TPCA and the black-oil model in GPRS. The TPCA results agree well with the ECLIPSE 100 simulation.

Fig. 3.4 shows the prediction of oil and gas production. Compared with ECLIPSE 100, GPRS with the TPCA model can get a better match than the GPRS using the black-oil model. The difference between the black-oil and the TPCA models in GPRS is significant when the gas phase disappears completely in gridblock (1,1,1), which takes place around 4000 days.

Let us study the injector gridblock (10,10,3). Because the pressure increases immediately, the gridblock stays in the one-phase region without any change in the bubble point. Therefore, there is no significant difference between the TPCA model and the black-oil model. The injection rate, pressure and saturation data are shown in Fig. 3.6 and Fig. 3.7.

### 3.4 Case 3: Gas Injection

Gas is injected with BHP control in this case for 6000 days. Since the reservoir is initially undersaturated, the oil can take up more gas if it is available. For gridblocks close to the injector, part of injected gas is dissolved in the oil, and the bubble point pressure increases correspondingly.

For the black-oil model with the fixed bubble point, the injected gas cannot dissolve in the oil because  $R_o$  does not change. So, the injected gas is modeled as a free phase and not allowed to dissolve in the oil. For gridblocks close to the producer, the block pressure decreases in the beginning because of depletion. Thus, free gas appears when the pressure is low enough. Then, the pressure increases and the gas phase goes in solution (disappears). After the gas breakthrough, free gas appears again. So, there is a complex sequence of gas-phase appearance and disappearance, which depends on the location and history of the gridblock under consideration. Associated with that are corresponding changes in the bubble-point pressure. Fig. 3.9

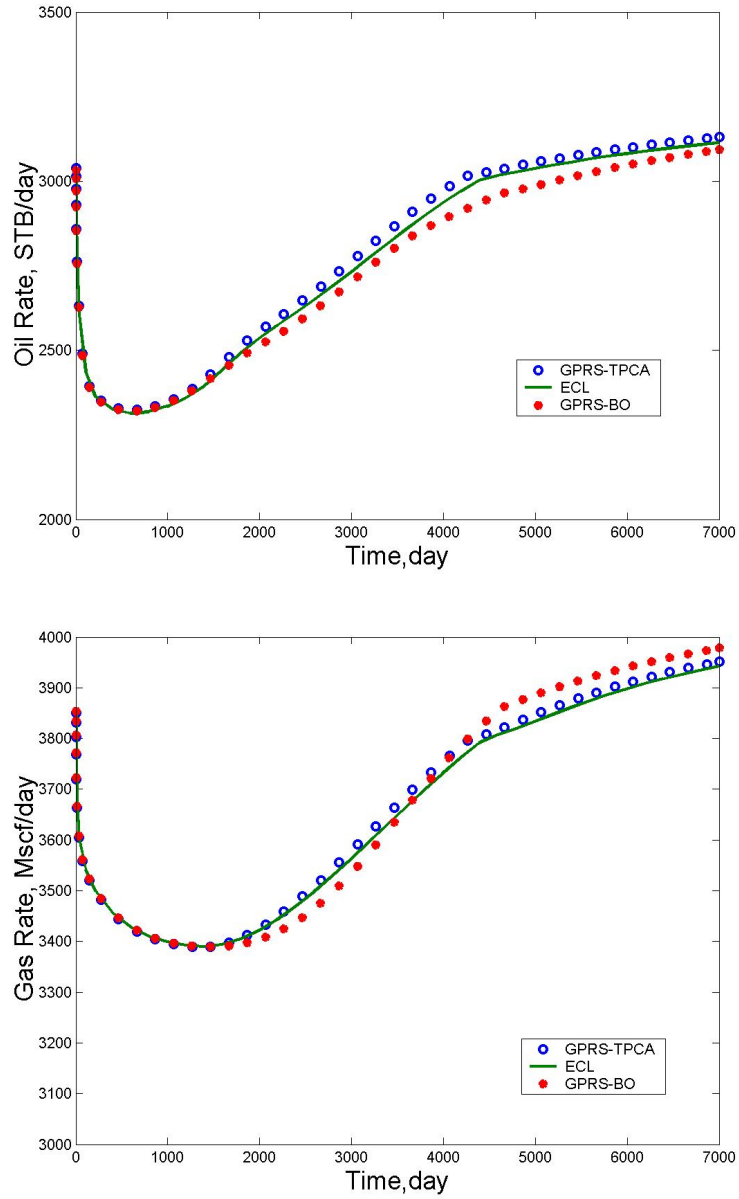


Figure 3.4: Oil and gas production rates [Case 2]

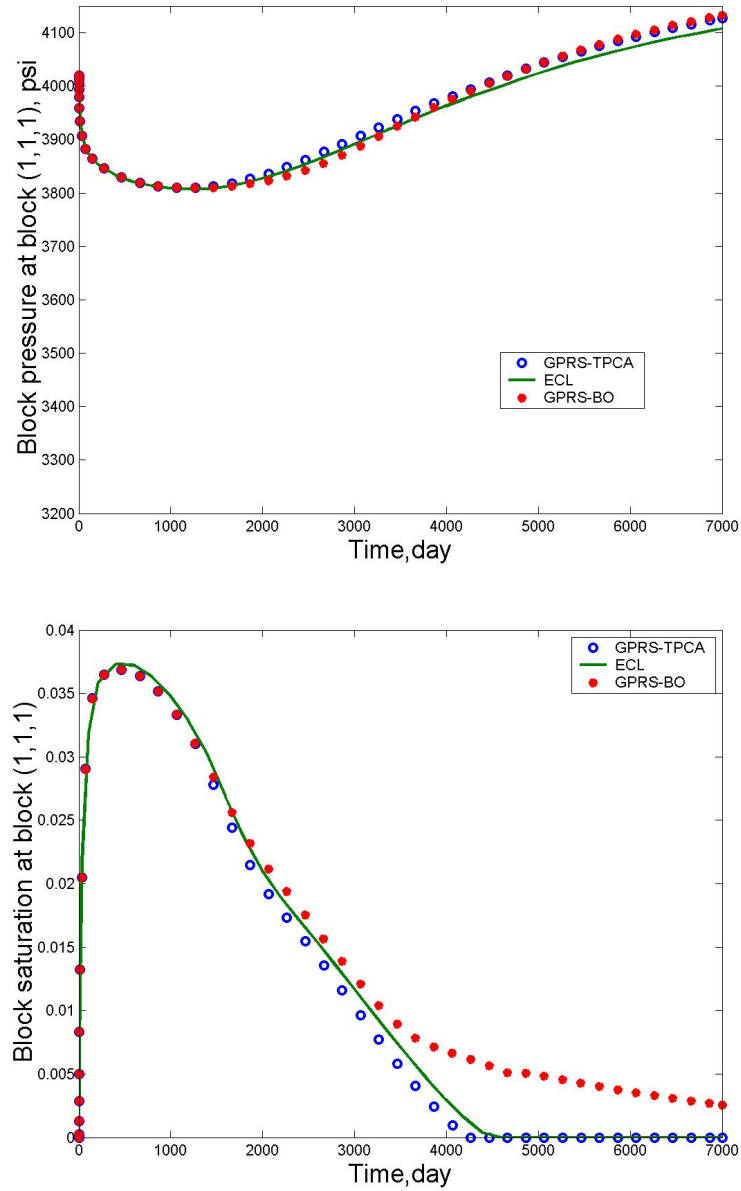


Figure 3.5:  $p$  and  $S_g$  at producer block (1,1,1) [Case 2]

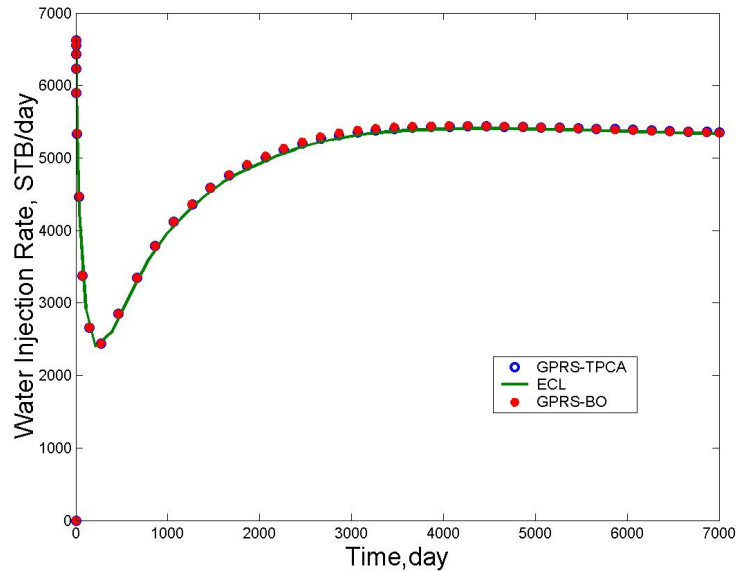


Figure 3.6: Water injection rate [Case 2]

shows that GPRS with TPCA models the process correctly. All the other figures (Fig. 3.8, Fig. 3.10 and Fig. 3.11) show perfect matches between ECLIPSE 100 and GPRS with TPCA.

### 3.5 Case 4: Alternate Water and Gas Injection

In this case, gas is injected for 500 days, then water is injected in the same well for the next 500 days. As explained in Section 3.3 and Section 3.4, the bubble point pressure increases in some gridblocks because of gas injection. In other gridblocks, on the other hand, the bubble point pressure decreases because of the release and subsequent migration of gas. The appearance/reappearance of the gas phase takes place throughout the flow process. The changes in the bubble point pressure are quite complicated in this test case. Fig. 3.12 shows the oil and gas production. ECLIPSE 100 and GPRS with the TPCA model give similar results. As expected, GPRS with the fixed bubble-point assumption leads to wrong predictions. Fig. 3.13 show matches

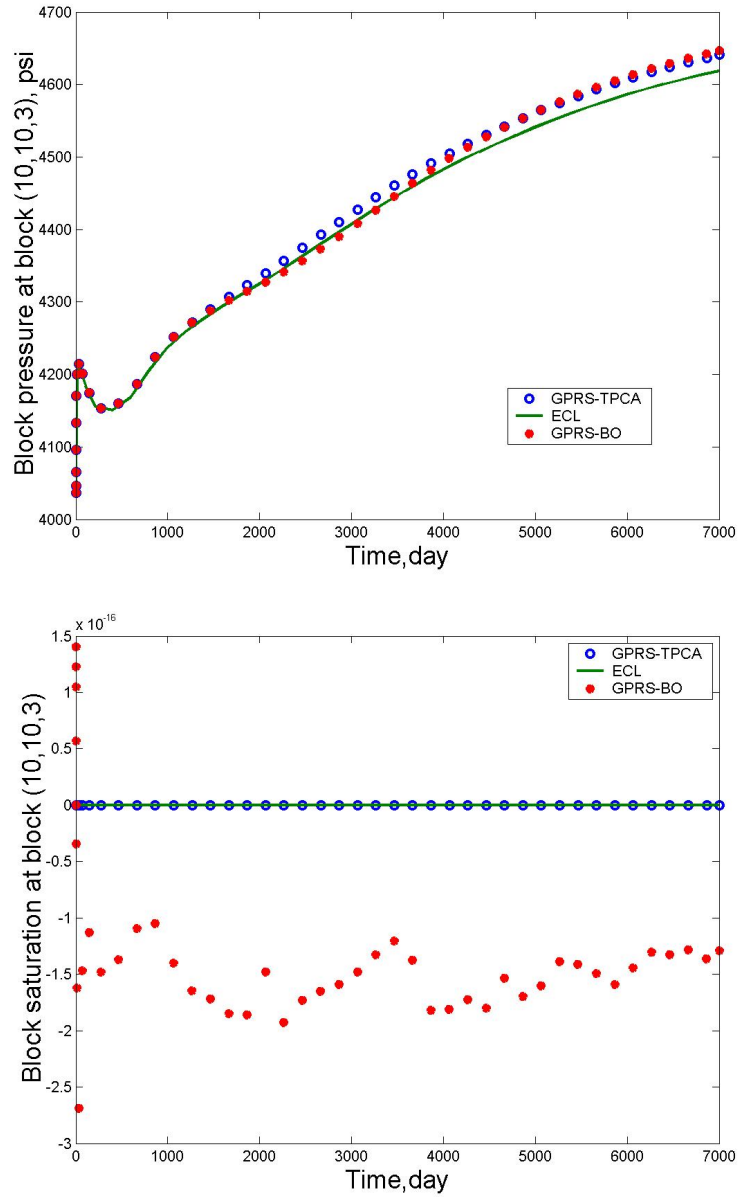


Figure 3.7:  $p$  and  $S_g$  at injector block (10,10,3) [Case 2]

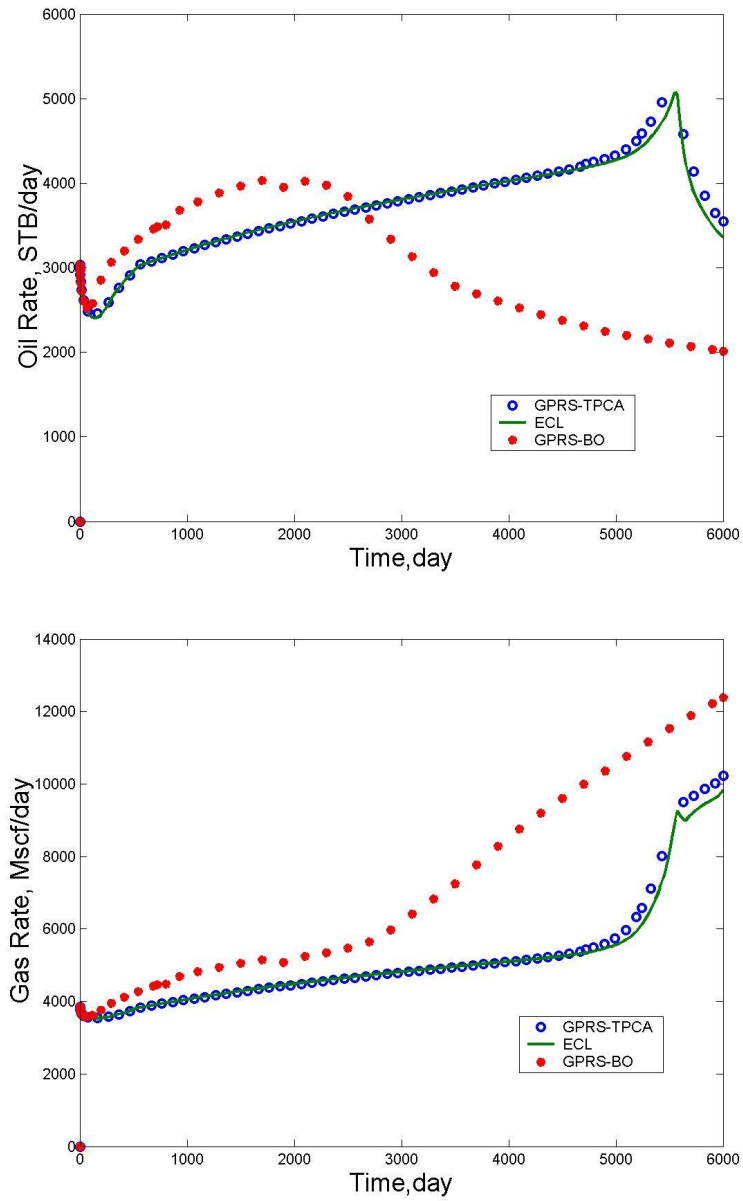


Figure 3.8: Oil and gas production rates [Case 3]

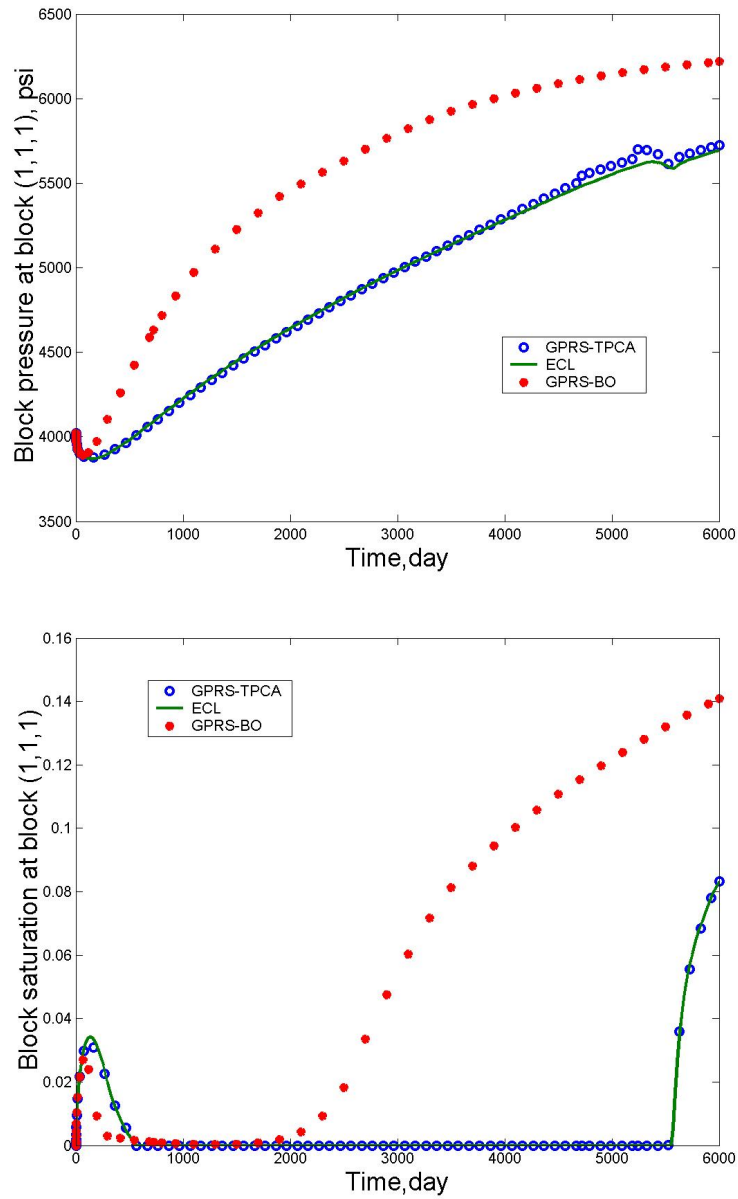


Figure 3.9:  $p$  and  $S_g$  at producer block (1,1,1) [Case 3]

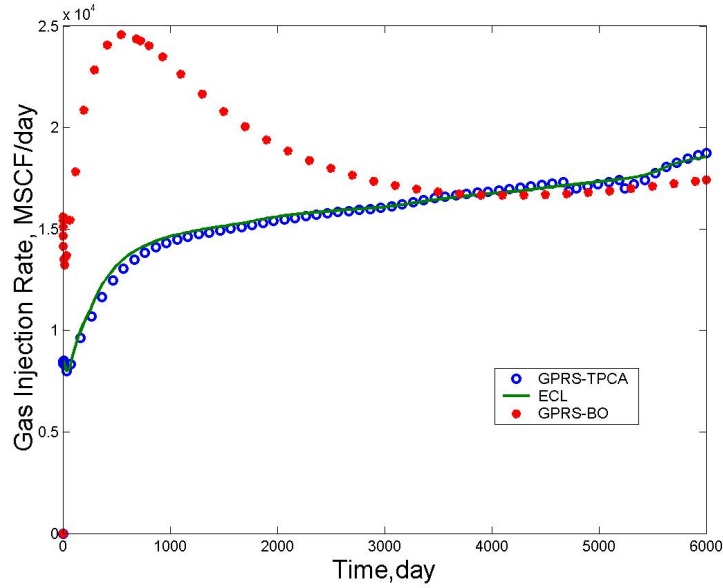
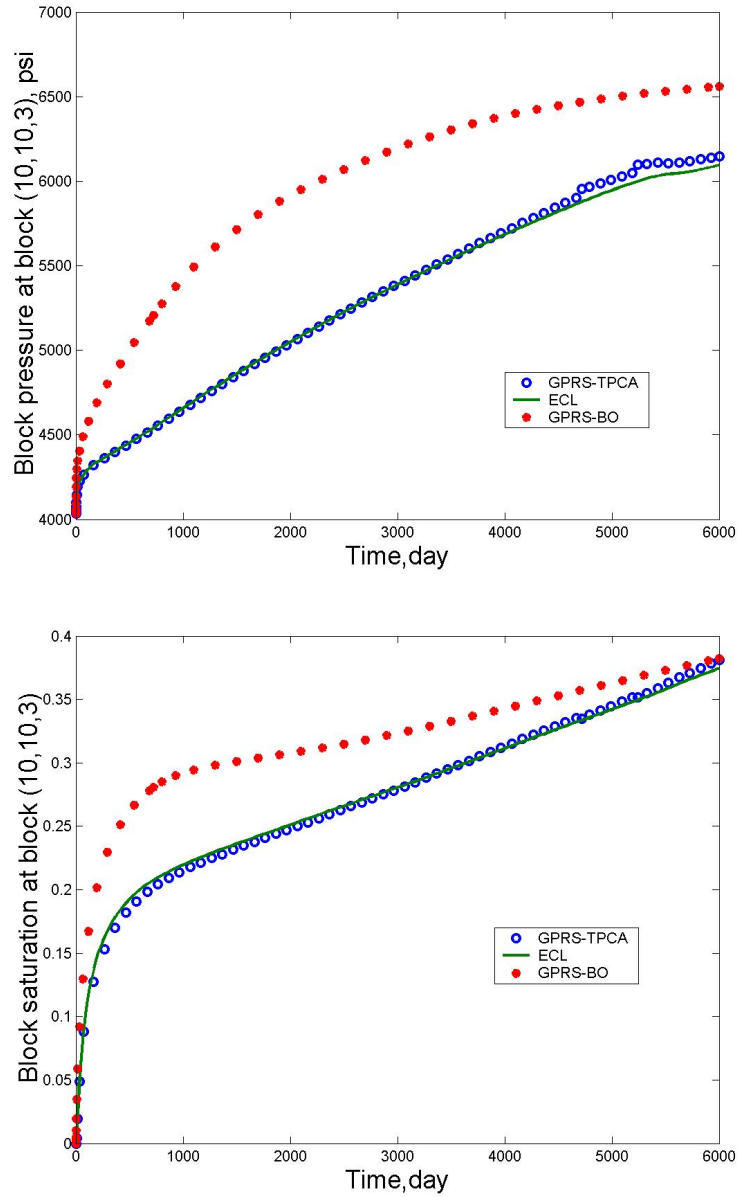


Figure 3.10: Gas injection rate [Case 3]

in the pressure and composition data. Fig. 3.14 and 3.15 show comparisons for the injector.

In this chapter, the TPCA model is verified using several test cases. These examples show different types of bubble-point variations in space and time. Compared with the black-oil model, the TPCA model implemented in GPRS gives much improved simulation results.



Figure 3.11:  $p$  and  $S_g$  at injector block (10,10,3) [Case 3]

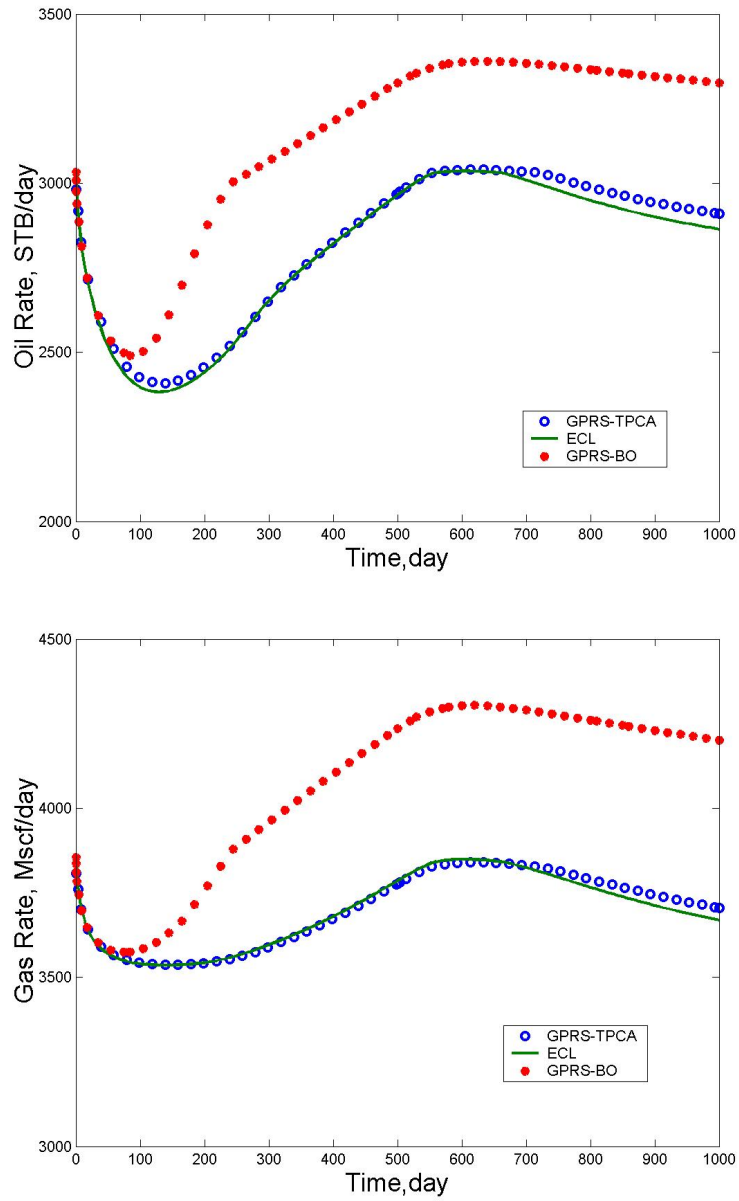


Figure 3.12: Oil and gas production rates [Case 4]

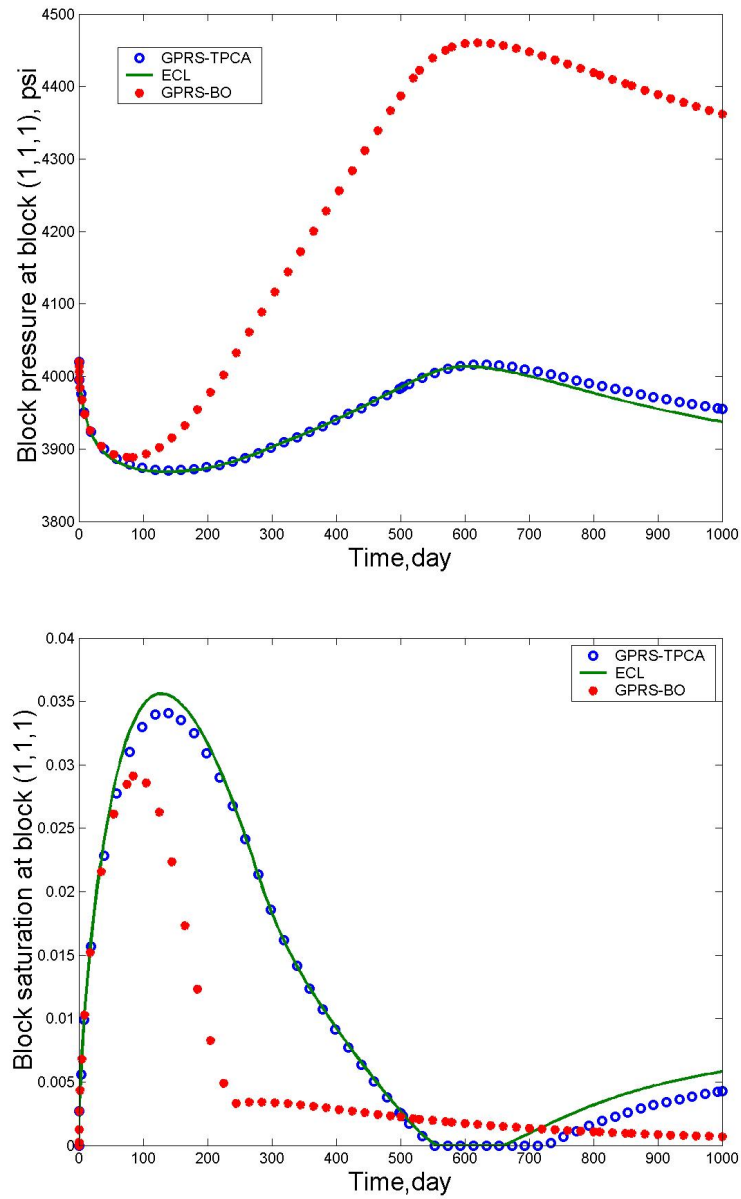


Figure 3.13:  $p$  and  $S_g$  at producer block (1,1,1) [Case 4]

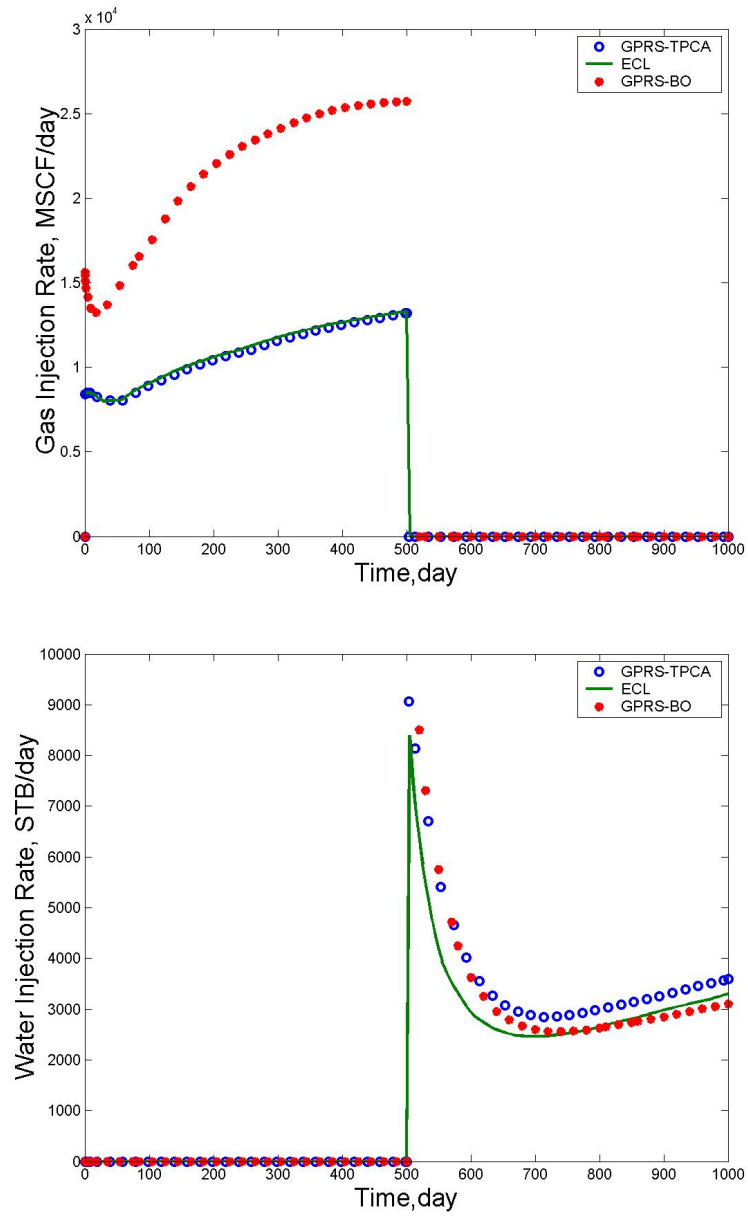
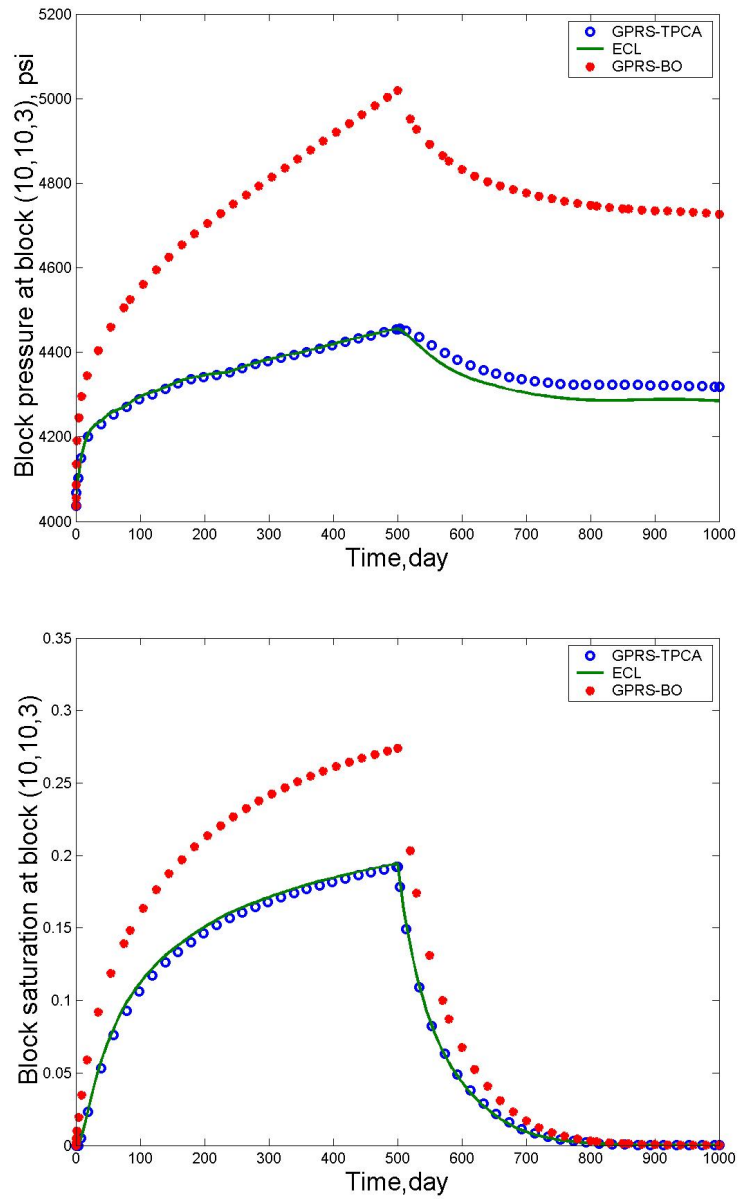


Figure 3.14: Gas and water injection rates [Case 4]

Figure 3.15:  $p$  and  $S_g$  at injector block (10,10,3) [Case 4]

# Chapter 4

## Conclusions and Future Work

In this work, GPRS is enhanced by adding a new fluid model to deal with black-oil simulations, where the bubble-point changes as a function of space and time. The Two Pseudo Component Approach (TPCA) [5] takes exactly the same input as the standard black-oil model, but it employs the compositional code base in GPRS to perform the simulation. The TPCA model is integrated into the GPRS framework and verified using several test cases through comparison with a commercial simulator. In these variable bubble-point problems, the black-oil model in GPRS, which is based on the assumption of a fixed bubble-point pressure, leads to significant errors. The TPCA model, on the other hand, is capable of solving these problems correctly and efficiently.

The TPCA framework, which makes full use of the robust variable switching strategy in the GPRS compositional model, was implemented for variable bubble-point problems only. We note here, however, that the TPCA framework is also applicable to problems with a variable dew-point. That is, with TPCA one can model a wide range of practical problems where the hydrocarbon mixture can be represented using two pseudo components, such as simple gas condensate systems.

The method to solve variable dew point problems is very similar to that used for variable bubble point problems. In the black-oil flash calculations, the following equilibrium rule can be used to determine the dew point

$$K_g/z_g + K_o/z_o = 1. \tag{4.1}$$

When the full capabilities of the TPCA framework are eventually implemented and integrated into the GPRS compositional code base, we can drop the standard black-oil branch.

# Nomenclature

$\bar{\rho}_{gst}$	gas molar density under standard condition, [mol/ft <sup>3</sup> ]
$\bar{\rho}_g$	gas molar density, [mol/ft <sup>3</sup> ]
$\bar{\rho}_{ost}$	oil molar density under standard condition, [mol/ft <sup>3</sup> ]
$\bar{\rho}_o$	oil molar density, [mol/ft <sup>3</sup> ]
$\bar{V}_g$	Molar fraction of gas phase
$\lambda_g$	gas mobility, [1/cp]
$\lambda_o$	oil mobility, [1/cp]
$\lambda_w$	water mobility, [1/cp]
$\phi$	porosity of rock
$\rho_g$	gas mass density, [lb/ft <sup>3</sup> ]
$\rho_o$	oil mass density, [lb/ft <sup>3</sup> ]
$B_g$	FVF, formation volume factor of dry gas, [RB/SCF]
$B_{wg}$	FVF, formation volume factor of wet gas, [RB/SCF]
$B_o$	FVF, formation volume factor of oil, [RB/STB]
$b_g$	reciprocal of dry gas FVF, [SCF/RB]
$b_o$	reciprocal of oil FVF, [STB/RB]



$b_{wg}$	reciprocal of wet gas FVF, [SCF/RB]
$BHP$	Bottom Hole Pressure in wellbore, [psi]
$d_x$	grid size in x direction, [ft]
$d_y$	grid size in y direction, [ft]
$d_z$	grid size in z direction, [ft]
$f_g^l$	gas liquid fugacity, [psi]
$f_g^v$	gas vapor fugacity, [psi]
$f_o^l$	oil liquid fugacity, [psi]
$f_o^v$	oil vapor fugacity, [psi]
$K_g$	K value of gas component
$K_o$	K value of oil component
$k_x$	permeability in x direction, [md]
$k_y$	permeability in y direction, [md]
$k_z$	permeability in z direction, [md]
$M_g$	gas component molecular weight, [lbm/lb-mol]
$M_o$	oil component molecular weight, [lbm/lb-mol]
$M_{pg}$	gas phase molecular weight, [lbm/lb-mol]
$M_{po}$	oil phase molecular weight, [lbm/lb-mol]
$n_h$	number of hydrocarbon components
$p$	grid block pressure, [psi]
$P^w$	well pressure, [psi]

$p_b$	bubble point pressure, [psi]
$p_g$	grid block gas phase pressure, [psi]
$P_i$	initial pressure in reservoir, [psi]
$p_o$	grid block oil phase pressure, [psi]
$p_w$	grid block water phase pressure, [psi]
$R_g$	GOR, Gas Oil Ratio, [SCF/STB]
$r_g$	gas oil ratio on molar basis
$R_o$	vaporized oil to gas ratio, [STB/SCF]
$r_o$	ratio of vaporized oil to free gas on molar basis, [STB/SCF]
$S_{gi}$	initial gas saturation
$S_g$	gas saturation
$S_{oi}$	initial oil saturation
$S_o$	oil saturation
$S_{wi}$	initial water saturation
$S_w$	water saturation
$T$	transmissibility between grid blocks, [md·ft]
$V$	volume of grid block, [ft <sup>3</sup> ]
$WI$	well index, [md·ft]
$x_g$	molar fraction of gas component in oil phase
$x_o$	molar fraction of gas component in oil phase
$y_g$	molar fraction of gas component in gas phase

$y_o$  molar fraction of oil component in gas phase

$z_g$  molar fraction of gas component

$z_o$  molar fraction of oil component

# Bibliography

- [1] Khalid Aziz and Antonin Settari. *Petroleum Reservoir Simulation*, Blitzprint Ltd, Calgary, Alberta, Canada, 1979
- [2] Hui Cao. Practical development of techniques for general purpose simulators, *Ph.D. Dissertation*, Stanford University, 2002
- [3] R.J. Steffensen and M. Sheffield. Reservoir simulation of a collapsing gas saturation requiring areal variation in bubble-point pressure. *SPE 4275, 3rd Symposium on Numerical Simulation of Reservoir Performance, Houston*, 1973
- [4] H. Kazemi. A reservoir simulator for studying productivity variation and transient behavior of a well in a reservoir undergoing gas evolution. *Trans. SPE of AIME*, 259, 1401-12 (JPT)
- [5] G.D. Shank and C.R. Vestal. Practical techniques in two-pseudo component black-oil simulation, *SPE15156*, 1989
- [6] Geoquest. Schlumberger, Eclipse 100 technical description 2005A, 2005
- [7] Geoquest. Schlumberger, Eclipse 100 reference manual 2005A, 2005
- [8] Aziz S. Odeh. Comparison of solutions to a three-dimensional black-oil reservoir simulation problem. *SPE 9723-PA*, JPT, Jan. 1981, pp13-25
- [9] Huanquan Pan. Implementation of fast phase equilibrium computations by lookup phase equilibrium constant K. *GPRS technical report*, Jan. 2007

- [10] G.D. Shank and C.R. Vestal. Supplement to SPE 15156, practical techniques in two-pseudo component black-oil simulation. *SPE 19119*, 1989
- [11] Lanmark graphics corporation. BlitzPak user's guide. 1998